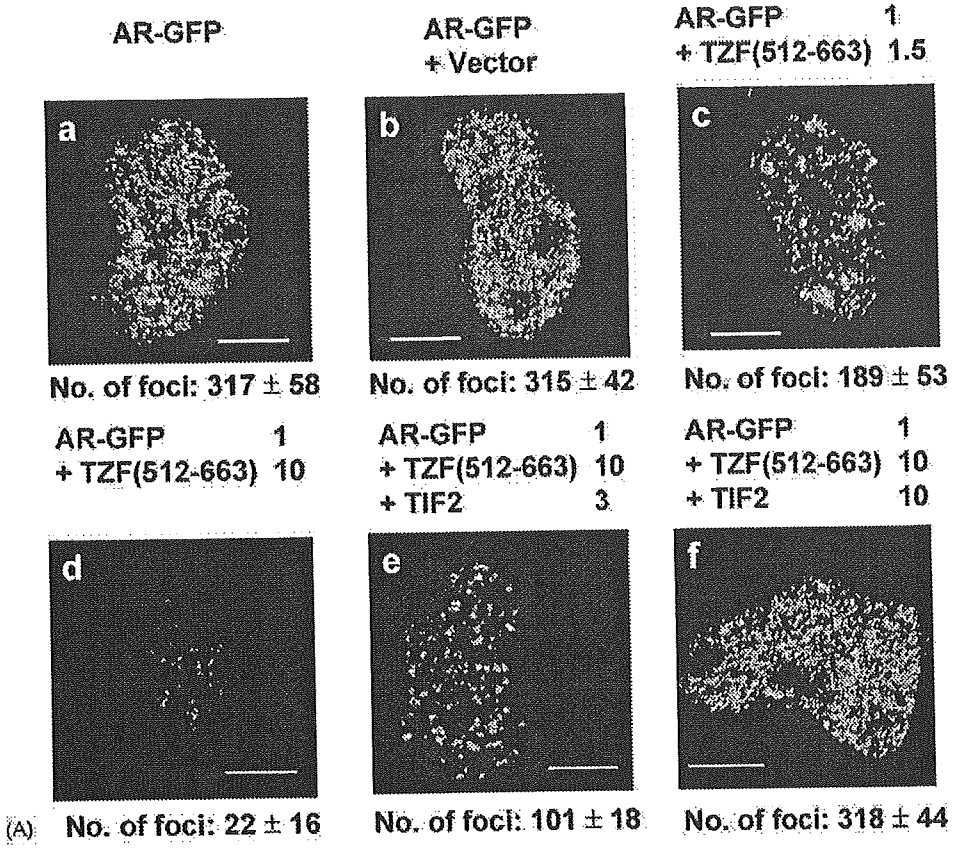

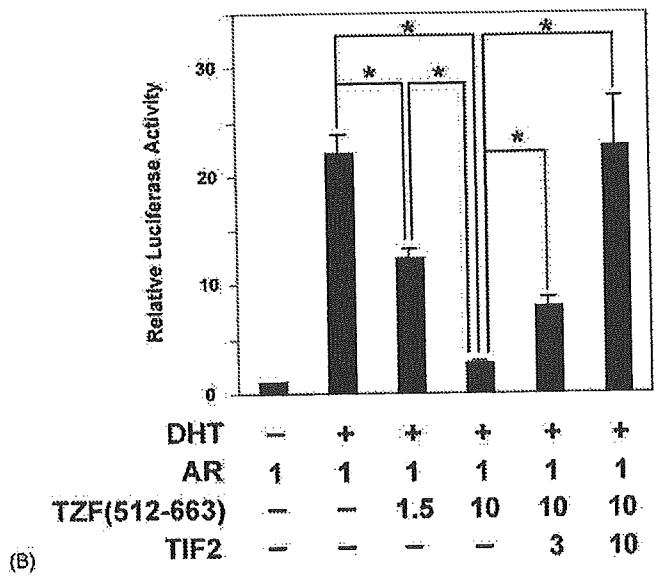

Fig. 8. The number of intranuclear AR foci is correlated with its transactivation activity. (A) Three-dimensional imaging analyses of the intranuclear AR foci. COS-7 cells were transiently transfected with 1 μg of pAR-GFP alone (a) or together with an empty vector (b), 1.5 μg of pFLAG-CMV2-TZF(512–663) (c), 10 μg of pFLAG-CMV2-TZF(512–663) (d), 10 μg of pFLAG-CMV2-TZF(512–663) and 3 μg of pcDNA-TIF2 (e) or 10 μg of pFLAG-CMV2-TZF(512–663) and 10 μg of pcDNA-TIF2 (f). The cells were incubated for 24 h and treated with 10 nM DHT for 1 h before observation. Two-dimensional tomographic images were collected by a confocal laser scanning microscope and reconstructed as described in Section 2. The number of subnuclear foci was calculated from at least 15 cells for each transfection and is shown as the mean ± S.D. below each panel. Bars = 5 μm. (B) Effects of TZF(512–663) and TIF2 on AR-mediated transcriptional activation. COS-7 cells were transiently transfected with 0.3 μg of pGL3-MMTV, 2 ng of pRL-CMV and 0.1 μg of pAR-GFP, together with various combinations of 0.15 or 1 μg of pFLAG-CMV2-TZF(512–663) and 0.3 or 1 μg of pcDNA-TIF2. After incubation with or without 10 nM DHT for 24 h, the cells were subjected to luciferase assays. Bars show the fold change in the luciferase activity relative to the value induced by AR without DHT. The data represent the means ± S.D. of three independent experiments. $^{*}P < 0.01$.

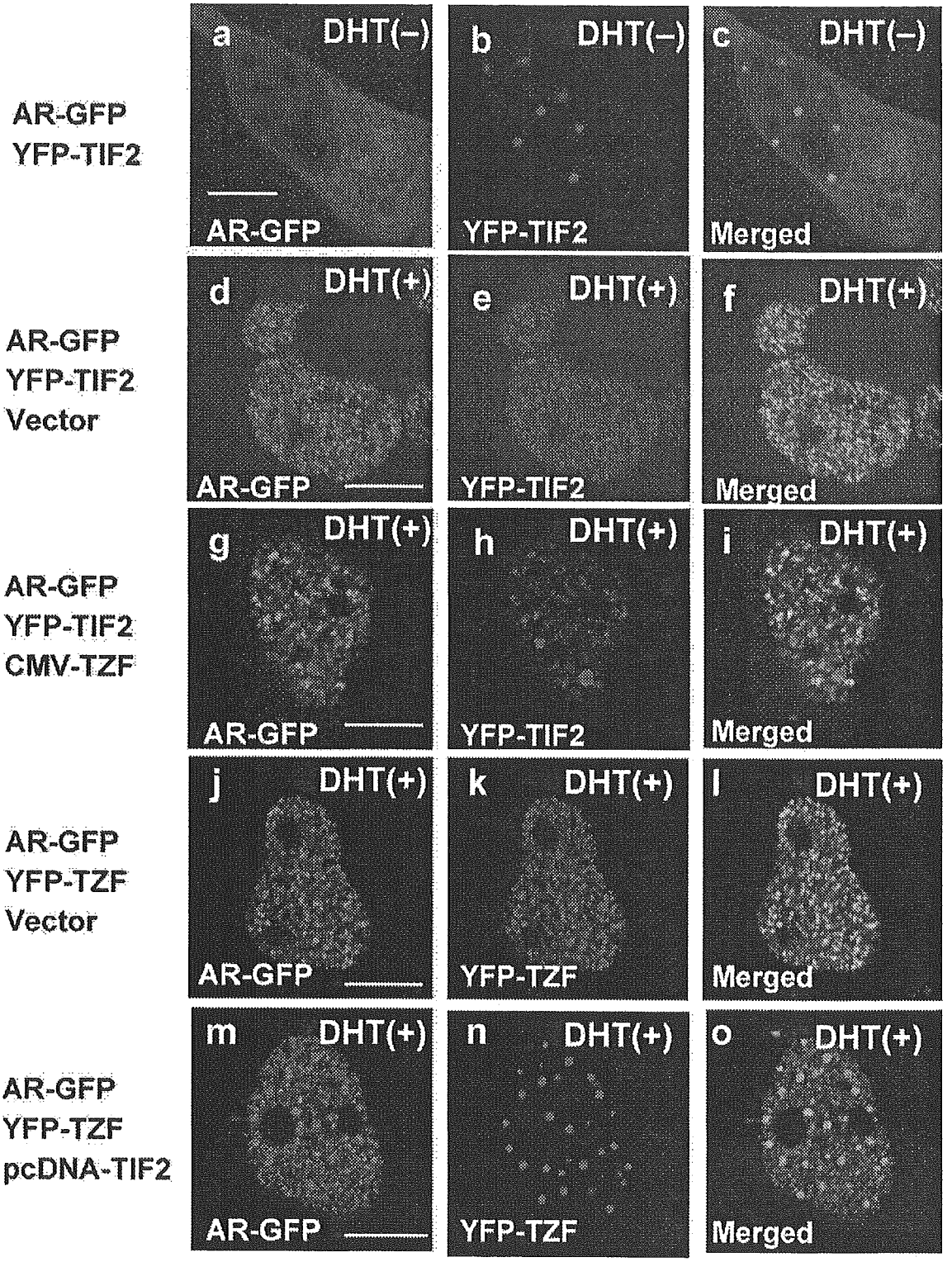

Fig. 9. Imaging analysis of the effects of TZF and TIF2 on the intranuclear foci formation of agonist-bound AR. (a–i) TZF releases TIF2 from intranuclear AR foci. COS-7 cells were transfected with 1 μg of pAR-GFP and 1.5 μg of pEYFP-TIF2 with (g–i) or without (a–f) 3 μg of pFLAG-CMV2-TZF, and incubated for 24 h. Prior to observation, the cells were incubated with (d–i) or without (a–c) 10 nM DHT for 1 h. Fluorescent signals were collected by a laser confocal microscope. AR signals (green; a, d and g), TIF2 signals (red; b, e and h) and merged signals (right; c, f and i) are shown. (j–o) TIF2 releases TZF from intranuclear AR foci. COS-7 cells were transfected with 1 μg of pAR-GFP and 2.2 μg of pEYFP-TZF with (m–o) or without (j–l) 3 μg of pcDNA-TIF2, and incubated for 24 h. After incubation with DHT for 1 h, the cells were observed by laser confocal microscopy. AR signals (green; j and m), TZF signals (red; k and n) and merged signals (right; l and o) are shown. Bars = 5 μm (for interpretation of the references to colour in this figure legend, the reader is referred to the web version of the article).

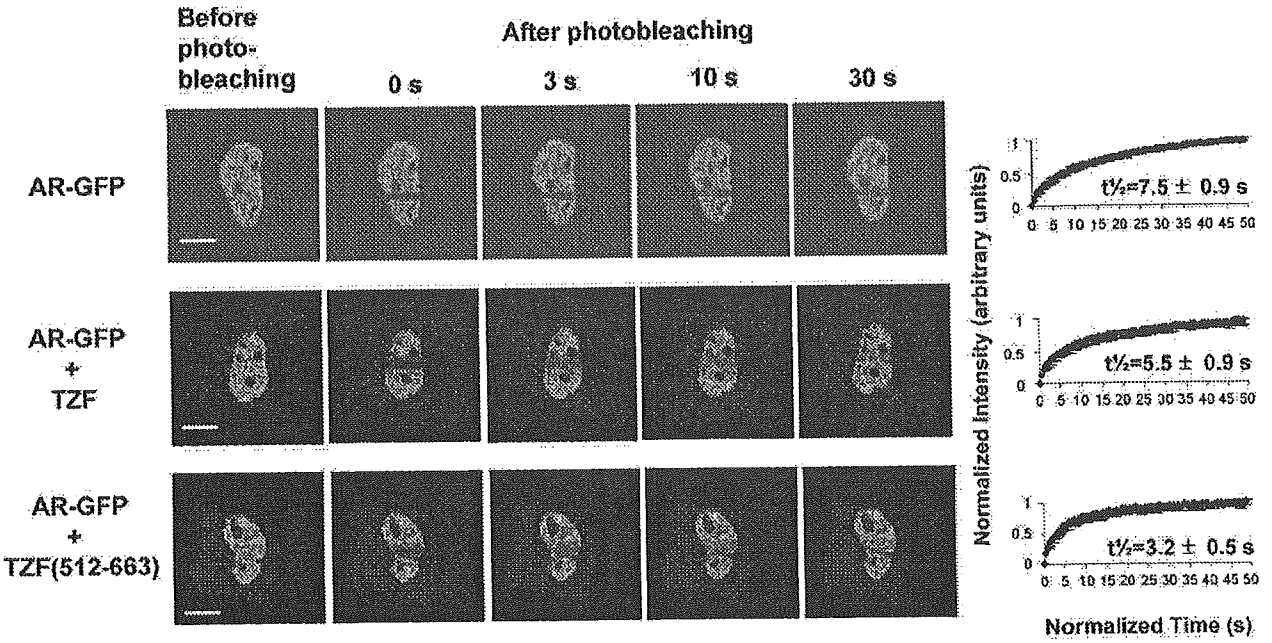

Fig. 10. Intranuclear mobility of AR coexpressed with or without TZF and TZF(512–663). COS-7 cells were transiently transfected with 1 μg of pAR-GFP alone (upper panels), 1 μg of pAR-GFP with 5 μg of pFLAG-CMV2-TZF (middle panels) or 1 μg of pAR-GFP with 5 μg of pFLAG-CMV2-TZF(512–663) (lower panels) as indicated. After incubation for 24 h, the cells were treated with 10 nM DHT for 1 h and subjected to FRAP analyses using a laser scanning microscope. A region of interest (ROI) in the nucleus was photobleached, and images were obtained before and at the indicated time points after the photobleaching. Bars = 5 μm. Graphs in the right panels show the recovery curves of the relative intensities in the photobleached ROI. The values of the half-recovery time ($t_{1/2}$) are expressed as means ± S.D. ($n = 15$).

are particularly abundant in eukaryotic proteomes and play an important role in biological processes, including protein–protein interactions (Liu et al., 2002; Liu and Rost, 2003). Therefore, further mutational analyses of TZF are necessary to identify the critical amino acid residues required for the repression of AR-mediated transactivation.

We applied the modified mammalian one-hybrid assay for detecting interactions of AR with the full-length TZF and its truncated mutants (Fig. 3). In this assay, expression of the TZF corepressor might cause an inhibition of basal AR-mediated transactivation. However, coexpression of AR with VP-16-fused TZF and its mutants induced strong transactivations due to the interaction between AR and TZF. These strong transactivations are thought to overcome the inhibitory effect by TZF.

Previous RT-PCR analyses revealed that TZF was highly expressed in the testes and moderately expressed in the prostate, adrenal glands, muscle, kidneys and uterus. During testicular development in mice, elevated expression of TZF was restricted to spermatocytes at the pachytene stage of meiotic prophase and to both round and elongated spermatids (Inoue et al., 2000; Ishizuka et al., 2003). This tissue- and stage-specific expression of TZF may indicate that TZF negatively regulates the actions of AR during development. However, the functions of TZF in vivo have not yet been clarified. Generation of *tzf*-deficient mice should provide strong clues toward elucidating the roles of TZF in developmental and physiological processes.

After ligand-binding, AR is translocated from the cytoplasm into the nucleus, where it activates the transcription of its target genes while simultaneously forming subnuclear foci (Tomura et al., 2001). This ligand-induced foci formation is commonly observed in steroid hormone receptors, such as glucocorticoid receptor (Ogawa et al., 1995), mineralocorticoid receptor (Fejes-Tóth et al., 1998), estrogen receptor-α (Stenoien et al., 2000; Htun et al., 1999) and vitamin D receptor (Racz and Barsony, 1999). Many pieces of evidence have accumulated indicating that this foci formation is closely linked to their transcriptional activation functions (Fejes-Tóth et al., 1998; Stenoien et al., 2000; Tomura et al., 2001; Saitoh et al., 2002). The present study provides another example, since GFP-TZF(512–663) was redistributed and colocalized with AR-CFP after addition of DHT, but distinct (complete) foci formation of AR-CFP was inhibited (Fig. 7E), reflecting the strong corepressor effect of TZF(512–663). However, quantitative analyses have hardly been carried out because it is difficult to count the numbers of intranuclear foci of steroid hormone receptors. We recently developed a three-dimensional imaging method that enables quantification of the numbers of intranuclear foci of steroid hormone receptors (Tomura et al., 2001; Saitoh et al., 2002). In the present study, the number of AR foci and AR-mediated transactivation were directly compared, and a clear correlation between these two factors was revealed (Fig. 8). N-CoR and SMRT are well-characterized corepressors that are thought to interact with nuclear receptors in the absence of a ligand or the presence of antagonists and confer transcriptional repression (Heinlein and Chang, 2002; Jones and Shi, 2003; Privalsky, 2004). However, AR was recently reported to be able to bind N-CoR and SMRT even in the presence of agonists (Cheng et al., 2002; Liao et al.,

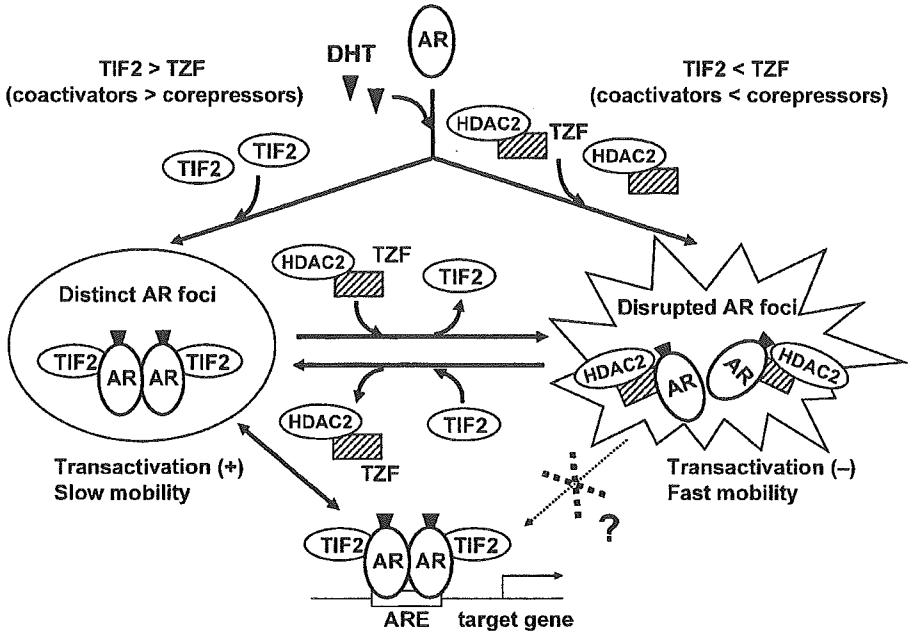

Fig. 11. An equilibrium model for intranuclear AR foci formation modulated by coregulators. The ratio of coactivators/corepressors expressed in a cell is presumed to determine the number of intranuclear foci and the transactivation activity of AR. Under the intranuclear condition where the content of corepressors such as TZF is considerably lower than that of coactivators, agonist-bound AR recruits coactivators and forms a transcriptionally active conformation, which is coupled with transfer to proper subnuclear compartments (distinct AR foci). AR foci formation is parallel to the transcription function and slow mobility. Agonist-bound AR in these proper compartments undergoes rapid exchange between the compartments and transcription sites of the target genes and is able to activate transcription. Under the condition where the content of corepressors is relatively higher than that of coactivators, the corepressors with HDAC bind to liganded AR, resulting in impairment of foci formation (disrupted AR foci). Agonist-bound AR in impaired compartments showed reduced transcriptional activation and fast mobility. It can be speculated that AR in the impaired foci might not have proper access to the transcription sites.

2003), and competition for agonist-bound AR between corepressors and coactivators was suggested to be the mechanism of the repression (Liao et al., 2003). A similar mechanism could be suggested for TZF-mediated repression of AR-induced transactivation, since the AR-mediated transactivation function varied depending on the TZF(512–663)/TIF2 ratio (Fig. 8B), while TZF was recruited by AR ligand-dependently, but also impaired complete foci formation of AR and dissociated the coactivator TIF2 from the AR foci (Fig. 9). However, an increase in TIF2 dissociated TZF and recovered the distinct foci formation of AR (Fig. 8A).

The FRAP analysis revealed that coexpression of full-length TZF or its mutants increased the intranuclear mobility of AR. Coexpression of TZF(512–663), which strongly repressed AR-mediated transcription, led to a higher mobility of AR compared to that of full-length TZF. The half-recovery time of AR would be correlated with its transcriptional activity. Previous studies revealed that ligand-bound steroid hormone receptors interact with the nuclear matrix, resulting in their decreased mobility (Fejes-Tóth et al., 1998; Htun et al., 1999; Schaaf and Cidlowski, 2003). TZF protein may inhibit the binding of AR to the nuclear matrix and cause a diffuse distribution of AR in the nucleus.

Our present results indicate that the ligand-dependent transactivation function of AR is quantitatively correlated with its foci formation, and that corepressors such as TZF act on these intranuclear events competitively with coactivators. Furthermore, the current results may suggest that competition with coactivators is a common repression mechanism for corepressors of agonist-bound AR, such as N-CoR, SMRT and TZF. Fig. 11 summarizes the speculated action of TZF based on the present findings.

Acknowledgements

We are grateful to Mitoshi Toki for his technical assistance in performing the three-dimensional imaging analyses. This work was supported in part by grants-in-aid for Scientific Research (B) and Exploratory Research and a grant for the 21st Century Center of Excellence (COE) Program (Kyushu University) from the Ministry of Education, Culture, Sports, Science and Technology, Japan.

References

Adachi, M., Takayanagi, R., Tomura, A., Imasaki, K., Kato, S., Goto, K., Yanase, T., Ikuyama, S., Nawata, H., 2000. Androgen-insensitivity syndrome as a possible coactivator disease. N. Engl. J. Med. 343, 856–862.

Aranda, A., Pascual, A., 2001. Nuclear hormone receptors and gene expression. Physiol. Rev. 81, 1269–1304.

Brinkmann, A.O., 2001. Molecular basis of androgen insensitivity. Mol. Cell. Endocrinol. 179, 105–109.

Cheng, S., Brzostek, S., Lee, S.R., Hollenberg, A.N., Balk, S.P., 2002. Inhibition of the dihydrotestosterone-activated androgen receptor by nuclear receptor corepressor. Mol. Endocrinol. 16, 1492–1501.

Fejes-Tóth, G., Pearce, D., Náray-Fejes-Tóth, A., 1998. Subcellular localization of mineralocorticoid receptors in living cells: effects of receptor agonists and antagonists. Proc. Natl. Acad. Sci. U.S.A. 95, 2973–2978.

Gelmann, E.P., 2002. Molecular biology of the androgen receptor. J. Clin. Oncol. 20, 3001–3015.

Gobinet, J., Poujol, N., Sultan, Ch., 2002. Molecular action of androgens. Mol. Cell. Endocrinol. 198, 15–24.

Gottlieb, B., Pinsky, L., Beitel, L.K., Trifiro, M., 1999. Androgen insensitivity. Am. J. Med. Genet. 89, 210–217.

Heinlein, C.A., Chang, C., 2002. Androgen receptor (AR) coregulators: an overview. Endocr. Rev. 23, 175–200.

Heinzel, T., Lavinsky, R.M., Mullen, T.M., Soderstrom, M., Laherty, C.D., Torchia, J., Yang, W.M., Brard, G., Ngo, S.D., Davie, J.R., Seto, E., Eisenman, R.N., Rose, D.W., Glass, C.K., Rosenfeld, M.G., 1997. A complex containing N-CoR, mSin3 and histone deacetylase mediates transcriptional repression. Nature 387, 43–48.

Htun, H., Holth, L.T., Walker, D., Davie, J.R., Hager, G.L., 1999. Direct visualization of the human estrogen receptor alpha reveals a role for ligand in the nuclear distribution of the receptor. Mol. Biol. Cell 10, 471–486.

Hu, X., Li, Y., Lazar, M.A., 2001. Determinants of CoRNR-dependent repression complex assembly on nuclear hormone receptors. Mol. Cell. Biol. 21, 1747–1758.

Inoue, A., Ishiji, A., Kasagi, S., Ishizuka, M., Hirose, S., Baba, T., Hagiwara, H., 2000. The transcript for a novel protein with a zinc finger motif is expressed at specific stages of mouse spermatogenesis. Biochem. Biophys. Res. Commun. 273, 398–403.

Ishizuka, M., Ohshima, H., Tamura, N., Nakada, T., Inoue, A., Hirose, S., Hagiwara, H., 2003. Molecular cloning and characteristics of a novel zinc finger protein and its splice variant whose transcripts are expressed during spermatogenesis. Biochem. Biophys. Res. Commun. 301, 1079–1085.

Ishizuka, M., Kawate, H., Takayanagi, R., Ohshima, H., Tao, R.-H., Hagiwara, H., 2005. A zinc finger protein TZF is a novel corepressor of androgen receptor. Biochem. Biophys. Res. Commun. 331, 1025–1031.

Jones, P.L., Shi, Y.-B., 2003. N-CoR-HDAC corepressor complexes: roles in transcriptional regulation by nuclear hormone receptors. Curr. Top. Microbiol. Immunol. 274, 237–268.

Kawano, H., Sato, T., Yamada, T., Matsumoto, T., Sekine, K., Watanabe, T., Nakamura, T., Fukuda, T., Yoshimura, K., Yoshizawa, T., Aihara, K., Yamamoto, Y., Nakamichi, Y., Metzger, D., Chambon, P., Nakamura, K., Kawaguchi, H., Kato, S., 2003. Suppressive function of androgen receptor in bone resorption. Proc. Natl. Acad. Sci. U.S.A. 100, 9416–9421.

Kawate, H., Wu, Y., Ohnaka, K., Nawata, H., Takayanagi, R., 2005. Tob proteins suppress steroid hormone receptor-mediated transcriptional activation. Mol. Cell. Endocrinol. 230, 77–86.

Kinyamu, H.K., Archer, T.K., 2004. Modifying chromatin to permit steroid hormone receptor-dependent transcription. Biochim. Biophys. Acta 1677, 30–45.

Liao, G., Chen, L.Y., Zhang, A., Godavarthy, A., Xia, F., Ghosh, J.C., Li, H., Chen, J.D., 2003. Regulation of androgen receptor activity by the nuclear receptor corepressor SMRT. J. Biol. Chem. 278, 5052–5061.

Liu, J., Rost, B., 2003. NORSp: predictions of long regions without regular secondary structure. Nucleic Acids Res. 31, 3833–3835.

Liu, J., Tan, H., Rost, B., 2002. Loopy proteins appear conserved in evolution. J. Mol. Biol. 322, 53–64.

Mangelsdorf, D.J., Thummel, C., Beato, M., Herrlich, P., Schütz, G., Umesono, K., Blumberg, B., Kastner, P., Mark, M., Chambon, P., Evans, R.M., 1995. The nuclear receptor superfamily: the second decade. Cell 83, 835–839.

Ogawa, H., Inouye, S., Tsuji, F.I., Yasuda, K., Umesono, K., 1995. Localization, trafficking, and temperature-dependence of the Aequorea green fluorescent protein in cultured vertebrate cells. Proc. Natl. Acad. Sci. U.S.A. 92, 11899–11903.

Ogryzko, V.V., Schiltz, R.L., Russanova, V., Howard, B.H., Nakatani, Y., 1996. The transcriptional coactivators p300 and CBP are histone acetyltransferases. Cell 87, 953–959.

Privalsky, M.L., 2004. The role of corepressors in transcriptional regulation by nuclear hormone receptors. Annu. Rev. Physiol. 66, 315–360.

Racz, A., Barsony, J., 1999. Hormone-dependent translocation of vitamin D receptors is linked to transactivation. J. Biol. Chem. 274, 19352–19360.

Roy, A.K., Lavrovsky, Y., Song, C.S., Chen, S., Jung, M.H., Velu, N.K., Bi, B.Y., Chatterjee, B., 1999. Regulation of androgen action. Vitam. Horm. 55, 309–352.

Saitoh, M., Takayanagi, R., Goto, K., Fukamizu, A., Tomura, A., Yanase, T., Nawata, H., 2002. The presence of both the amino- and carboxyl-terminal domains in the AR is essential for the completion of a transcriptionally active form with coactivators and intranuclear compartmentalization common to the steroid hormone receptors: a three-dimensional imaging study. Mol. Endocrinol. 16, 694–706.

Schaaf, M.J.M., Cidlowski, A., 2003. Molecular determinants of glucocorticoid receptor mobility in living cells: the importance of ligand affinity. Mol. Cell. Biol. 23, 1922–1934.

Stenoien, D.L., Mancini, M.G., Patel, K., Allegretto, E.A., Smith, C.L., Mancini, M.A., 2000. Subnuclear trafficking of estrogen receptor-alpha and steroid receptor coactivator-1. Mol. Endocrinol. 14, 518–534.

Stenoien, D.L., Patel, K., Mancini, M.G., Dutertre, M., Smith, C.L., O'Malley, B.W., Mancini, M.A., 2001. FRAP reveals that mobility of oestrogen receptor-alpha is ligand- and proteasome-dependent. Nat. Cell. Biol. 3, 15–23.

Tomura, A., Goto, K., Morinaga, H., Nomura, M., Okabe, T., Yanase, T., Takayanagi, R., Nawata, H., 2001. The subnuclear three-dimensional image analysis of androgen receptor fused to green fluorescence protein. J. Biol. Chem. 276, 28395–28401.

Webb, P., Anderson, C.M., Valentine, C., Nguyen, P., Marimuthu, A., West, B.L., Baxter, J.D., Kushner, P.J., 2000. The nuclear receptor corepressor (N-CoR) contains three isoleucine motifs (I/LXXII) that serve as receptor interaction domains (IDs). Mol. Endocrinol. 14, 1976–1985.

Yanase, T., Adachi, M., Goto, K., Takayanagi, R., Nawata, H., 2004. Coregulator-related diseases. Intern. Med. 43, 368–373.

Yeh, S., Tsai, M.Y., Xu, Q., Mu, X.M., Lardy, H., Huang, K.E., Lin, H., Yeh, S.D., Altuwaijri, S., Zhou, X., Xing, L., Boyce, B.F., Hung, M.C., Zhang, S., Gan, L., Chang, C., 2002. Generation and characterization of androgen receptor knockout (ARKO) mice: an in vivo model for the study of androgen functions in selective tissues. Proc. Natl. Acad. Sci. U.S.A. 99, 13498–13503.

Available online at www.sciencedirect.com
SCIENCE DIRECT
ELSEVIER
Biochemical and Biophysical Research Communications 341 (2006) 515–521
BBRC
www.elsevier.com/locate/ybbrc

Opposite effects of alternative TZF spliced variants on androgen receptor

Rong-Hua Tao [a], Hisaya Kawate [a], Keizo Ohnaka [a], Masamichi Ishizuka [b], Hiromi Hagiwara [b], Ryoichi Takayanagi [a,*]

[a] *Department of Geriatric Medicine, Graduate School of Medical Sciences, Kyushu University, Maidashi 3-1-1, Higashi-ku, Fukuoka 812-8582, Japan*
[b] *Department of Biomedical Engineering, Toin University of Yokohama, Kurogane-cho 1614, Aoba-ku, Yokohama 225-8502, Japan*

Received 28 December 2005
Available online 13 January 2006

Abstract

We previously demonstrated that testicular zinc-finger protein (TZF) was a corepressor of the androgen receptor (AR). In the present study, we further showed that TZF-L, an alternative spliced variant of TZF, enhanced transactivation function of AR. Deletion analysis of TZF-L revealed that its N-terminus, which almost corresponded to that of TZF, but not its C-terminus was able to interact with AR. Additional analysis suggested that TZF and TZF-L were able to form both homodimers and heterodimers. TZF-L inhibited the homodimer formation of TZF and the intranuclear dot formation of TZF. We propose that in the unique regulation system of AR-mediated transactivation, two spliced isoforms of TZF act as coactivator and corepressor, respectively.

Keywords: Androgen receptor; Transcription; Coregulator; GFP

Androgens play essential roles in the expression of the male phenotype through the androgen receptor (AR). AR is a member of the nuclear receptor (NR) superfamily, which generally functions as a ligand-dependent transcriptional factor [1,2]. AR is located in the cytoplasm before ligand binding and becomes translocated into the nucleus upon ligand binding to recognize androgen responsive elements of target genes, resulting in transcriptional activation or repression [1,3,4]. We previously reported that AR formed intranuclear fine foci in a ligand-dependent manner [5,6]. NR-mediated transcription is known to be regulated by two types of cofactors, coactivators and corepressors. To date, a large number and a wide variety of coactivators and corepressors of NR-mediated transactivation have been identified [7,8].

TZF (testicular zinc-finger protein) consists of 942 amino acid residues and carries a Cys_2-His_2 type of zinc-finger motif at the C-terminal end of the protein [9]. TZF-L has been identified as an alternative spliced variant of TZF. It has 2025 amino acid residues, and the N-terminal 902 amino acids of TZF-L protein are identical to those of TZF [10]. TZF-L has two zinc-finger motifs of the Cys_2-His_2 type, one of which is common with that of TZF. Both TZF and TZF-L are highly expressed in testes and moderately in kidneys and ovaries. We previously reported that TZF repressed AR-mediated transcriptional activation by interacting with the N-terminus of AR [11]. TZF forms intranuclear dots and is recruited into AR foci after treatment of the ligand.

In the present study, we investigated effects of TZF-L on AR-mediated transactivation function. In contrast with TZF, TZF-L enhanced AR-mediated transcriptional activation. The N-terminus of TZF-L, which almost corresponds to TZF, was able to interact with AR. We also indicated that TZF and TZF-L formed both homodimers and heterodimers. These two spliced variants of TZF may have unique regulation mechanisms for AR-mediated transcriptional activation.

* Corresponding author. Fax: +81 92 642 6911.
E-mail address: takayana@geriat.med.kyushu-u.ac.jp (R. Takayanagi).

0006-291X/$ - see front matter © 2006 Elsevier Inc. All rights reserved.
doi:10.1016/j.bbrc.2005.12.213

Materials and methods

Plasmid constructs. Expression plasmids for AR, pCMV-hAR, and firefly reporter plasmids (pGL3-MMTV and pGL3-PSA) were prepared as previously described [5,11,12]. Expression plasmids for TZF-L, pLP-EGFP-C1-TZF-L [10] were digested with *Sal*I and *Xho*I restriction enzymes to obtain a *Sal*I–*Xho*I fragment encoding the C-terminus of TZF-L, and a *Sal*I fragment encoding the remaining portion of TZF-L. The *Sal*I–*Xho*I fragment was first inserted into the *Sal*I site of both pEGFP-C1 and pEYFP-C1 vectors (BD Sciences Clontech, Palo, Alto, CA), followed by insertion of the *Sal*I fragment into the *Sal*I site of the same vector to produce pEGFP-TZF-L and pEYFP-TZF-L, respectively. Similarly, another expression plasmid for TZF-L, pFLAG-CMV2-TZF-L, was constructed using pFLAG-CMV2 vector (Sigma–Aldrich, St. Louis, MO). An expression plasmid for the N-terminus (amino acids 1–902) of TZF-L, pEGFP-TZF-L-N, was constructed as follows: a fragment encoding 758–902 amino acid residues of TZF-L was amplified by PCR from pLP-EGFP-C1-TZF-L, using the following set of oligonucleotide primers: TZF-L-N-5 (5′-GTGAGTCGACTTCAGGAT-3′) and TZF-L-N-3 (5′-CCGCTCGAGCTGTGTGTGCTTCTTATTGTGC-3′). The PCR-amplified fragment was cloned into pCR-Blunt II-TOPO vector (Invitrogen Corp., Carlsbad, CA), and the *Sal*I–*Xho*I fragment encoding TZF-L (amino acids 758–902) was subcloned into the *Sal*I site of pEGFP-C1 vector, followed by insertion of the *Sal*I fragment encoding the N-terminus (amino acids 1–758) of TZF-L into the *Sal*I site. To construct an expression plasmid for TZF-L-C (amino acids 902–2025), pEGFP-TZF-L-C, a fragment encoding amino acid residues 902–1171 of TZF-L was amplified by PCR from pLP-EGFP-C1-TZF-L using the following set of primers: TZF-L-C-5 (5′-CCGCTCGAGAGACACTGGATCCCTAC AAC-3′) and TZF-L-C-3 (5′-AACCTGACTTGCGGAGTACTG-3′). The PCR-amplified fragment was cloned into pCR-Blunt II-TOPO vector, and then an *Xho*I–*Eco*RI fragment encoding TZF-L (amino acids 902–1171) was subcloned into the *Xho*I and *Eco*RI sites of pEGFP-C1 vector, followed by insertion of the *Sca*I–*Xho*I fragment of pLP-EGFP-C1-TZF-L encoding the C-terminus (amino acids 1171–2025) of TZF-L into the *Sca*I and *Sal*I sites. The TZF cDNA fragment was subcloned into pFLAG-CMV2 and pEGFP-C1, resulting in pFLAG-CMV2-TZF and pEGFP-C1-TZF, respectively.

For the mammalian two-hybrid assay, pEGFP-TZF-L was digested with *Sma*I, and a *Sma*I fragment containing TZF-L cDNA was inserted into blunt-ended *Bam*HI sites of pBIND and pACT vectors (Promega, Madison, WT), to produce pBIND-TZF-L and pACT-TZF-L, respectively. Expression plasmids for TZF-L-C, pBIND-TZF-L-C, and pACT-TZF-L-C were constructed by inserting the *Xho*I–*Sma*I fragment from pEGFP-TZF-L-C into *Sal*I- and *Eco*RV-digested pBIND, and pACT vectors, respectively. Expression plasmids for TZF-L-N, pBIND-TZF-L-N, and pACT-TZF-L-N were constructed by inserting a *Kpn*I fragment from pEGFP-TZF-L-N into *Kpn*I sites of pBIND and pACT vectors. The cDNA fragment of TZF was subcloned into pBIND and pACT vectors to produce pBIND-TZF and pACT-TZF, respectively. Expression plasmid for AR, pACT-AR, was prepared as previously described [13]. Validity of the structure of all constructs was confirmed by DNA sequencing.

Cell culture. The monkey kidney-derived cell line COS-7 was obtained from the Riken Cell Bank (Tokyo, Japan). The human prostatic cancer cell line PC3 and the mouse fibroblast cell line NIH3T3 were obtained from the American Type Culture Collection (Manassas, VA). COS-7 and NIH3T3 cells were maintained in Dulbecco's modified Eagle's medium (DMEM, Sigma), and PC3 cells were maintained in Roswell Park Memorial Institute 1640 medium (Sigma), supplemented with 10 % fetal bovine serum (FBS, Sanko Junyaku, Tokyo, Japan) and 100 U/ml penicillin–streptomycin (Invitrogen).

Functional reporter assay. Cells were cultured in 12-well plates (1×10^5 cells/well), and transfected with 0.3 μg/well pGL3-PSA or pGL3-MMTV as reporter, 2 ng/well pRL-CMV (Renilla Luciferase vector, Promega, Madison, WI) as internal control, and 0.1 μg/well pCMV-hAR together with 0.5 μg/well of the expression plasmid for TZF or TZF-L, using 2.7 μl Superfect Transfection Reagent (Qiagen GmbH, Hilden, Germany). In all co-transfection studies, the total amount of plasmid DNA was fixed by adjusting the transfection mixture with empty vector. After 4-h incubation, cells were rinsed with phosphate-buffered saline (PBS), and re-fed with medium containing 10% charcoal-stripped FBS, in the presence or absence of 10 nM 5α-dihydrotestosterone (DHT). After an additional incubation for 24 h, cells were lysed using lysis buffer supplied with the luciferase kit (Promega), and luciferase activity was assayed using the Dual-Luciferase Reporter Assay System (Promega). Data were expressed as means ± SD of three independent experiments. One-way analysis of variance followed by Scheffé's test was used for multigroup comparisons. A P value <0.05 was considered to be statistically significant.

Mammalian two-hybrid assay. NIH3T3 (1×10^5 cells/well) cells were seeded in 12-well plates at 24 h before transfection. Cells were co-transfected with 0.6 μg pG5*luc* (Promega) as reporter, 0.3 μg pACT-AR and 0.1 μg pBIND-TZF-L, pBIND-TZF-L-N or pBIND-TZF-L-C. The pBIND vector also encoded the *Renilla reniformis* luciferase as internal control. For detection of homodimers and heterodimers, plasmids (pG5*luc*, pACT-TZF, pBIND-TZF, pACT-TZF-L, and pBIND-TZF-L) were used for transfection. Equimolar amounts of the empty vector DNA were added to each well. Following treatment with 10 nM DHT for 24 h, cells were lysed, and luciferase activity was measured as described above.

Co-immunoprecipitation and immunoblot analysis. COS-7 cells (1×10^6 cells/dish) were seeded in 100-mm culture dishes, and transiently transfected with 1.5 μg pCMV-hAR using 7.5 μg pEGFP-TZF-L, 5 μg pEGFP-TZF-L-N, and 5 μg pEGFP-TZF-L-C, followed by 24-h incubation in the presence of 10 nM DHT. Whole cell lysates were prepared by lysing cells in a buffer consisting of 20 mM Hepes–NaOH, pH 7.9, 20% glycerol, 100 mM KCl, 0.2 mM EDTA, 0.5% NP-40, and one tablet of protease inhibitor cocktail (Roche Diagnostics, Tokyo, Japan) for 30 min at 4 °C, followed by brief sonication and centrifugation. Protein concentrations were measured using a BCA protein assay kit (Pierce, Rockford,

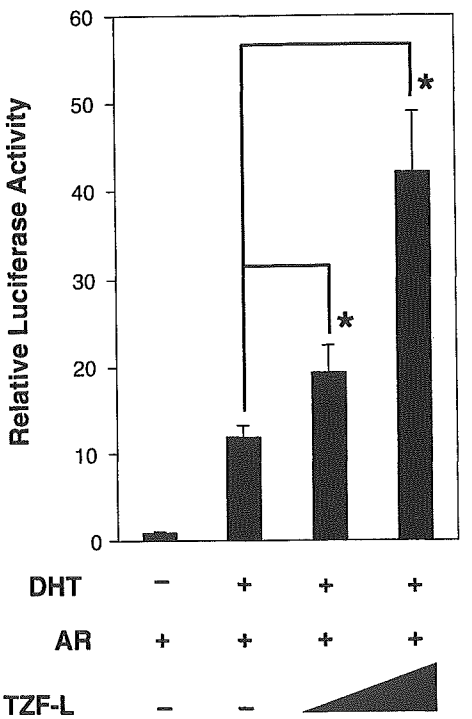

Fig. 1. TZF-L enhances AR-mediated transcriptional activation. PC3 cells were transfected with pGL3-PSA, pRL-CMV, and pCMV-hAR together with or without pFLAG-CMV2-TZF-L as described in Materials and methods. Molar ratios of transfected amounts of pCMV-hAR and pFLAG-CMV2-TZF-L were 1:5 or 1:10. Cells were treated with or without 10 nM DHT for 24 h, and luciferase activity was measured. Bars represent fold changes in luciferase activity relative to the value by AR without DHT. $^*P < 0.01$.

IL), and each protein concentration was adjusted to 1 mg/ml. For the immunoprecipitation assay, antibodies against GFP or AR (C-19, Santa Cruz Biotechnology, Santa Cruz, CA) were pre-incubated with protein A magnetic beads (New England Biolabs, Beverly, MA) at 4 °C for 2 h. Each lysate (200 μg) was incubated with 10 μg anti-GFP or anti-AR antibody-conjugated beads in WB buffer (20 mM Hepes–NaOH, pH 7.9, 20% glycerol, 100 mM KCl, 0.2 mM EDTA, 0.5% NP-40, and 0.5% skim milk) at 4 °C overnight. After the beads were washed three times with 180 μl WB buffer, the bound proteins were eluted in 2 × sodium dodecyl sulfate–polyacrylamide gel electrophoresis (SDS–PAGE) sample buffer (2% SDS, 100 mM dithiothreitol, 60 mM Tris–HCl, pH 6.8, and 0.01% bromophenol blue) and subjected to 10% SDS–PAGE at 20 mA for 5 h. An immunoblot analysis was then performed as previously described [14], using the anti-AR (C-19) antibody for AR, anti-TZF antibody for TZF, and anti-GFP antibody for GFP-fused TZF-L and its mutants.

Confocal laser scanning microscopy. For living cell microscopy, COS-7 cells (2×10^5 cells/dish) were cultured in 35-mm glass-bottomed dishes (Asahi Techno Glass, Tokyo, Japan) and transfected with pEGFP-TZF and/or pEYFP-TZF-L, or pFLAG-CMV2-TZF-L using Superfect reagents (Qiagen). After 3-h incubation, cells were washed with PBS, followed by incubation in DMEM supplemented with 10% charcoal-treated FBS for 16–20 h. Cells were observed with an Axiovert 200 M inverted microscope, equipped with an LSM 510 META scan head (Carl Zeiss, Jena, Germany), and using a 100 × 1.4 numerical aperture oil

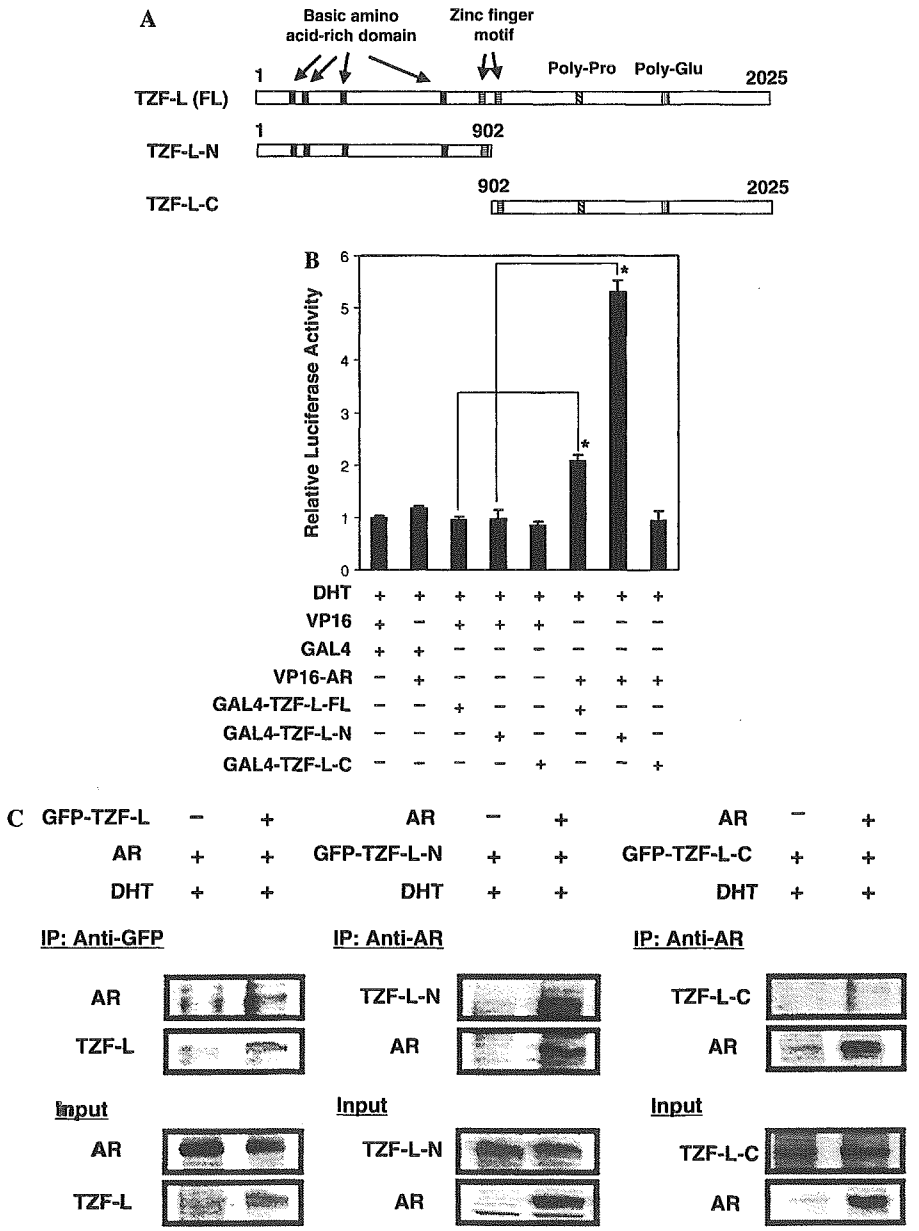

Fig. 2. Identification of the interaction between TZF-L and AR. (A) Schematic representation of full-length TZF-L and its truncated mutants, TZF-L-N and TZF-L-C. (B) A mammalian two-hybrid assay indicated interactions of the full length TZF-L and its N-terminus with AR. NIH3T3 cells were co-transfected with pG5*luc*, pACT-AR, and pBIND-TZF-L, pBIND-TZF-L-N or pBIND-TZF-L-C, and luciferase activities were measured after treatment with 10 nM DHT for 24 h, as described in Materials and methods. Bars represent fold changes in luciferase activity relative to the value by the empty vectors. Data are expressed means ± SD of three independent experiments. $^*P < 0.01$. (C) Co-immunoprecipitation analyses of TZF-L and its truncated mutants with AR. COS-7 cells were transfected with pCMV-hAR with pEGFP-TZF-L, pEGFP-TZF-L-N or pEGFP-TZF-L-C and then incubated with 10 nM DHT for 24 h as described in Materials and methods. Whole cell lysates were immunoprecipitated using anti-GFP or anti-AR antibody. Then, precipitates were subjected to immunoblot analysis using the anti-AR antibody for detection of AR, and the anti-GFP antibody for detections of TZF-L, TZF-L-N, and TZF-L-C. Whole cell lysates were also subjected to immunoblot analysis to confirm expressions of AR, TZF-L, TZF-L-N, and TZF-L-C.

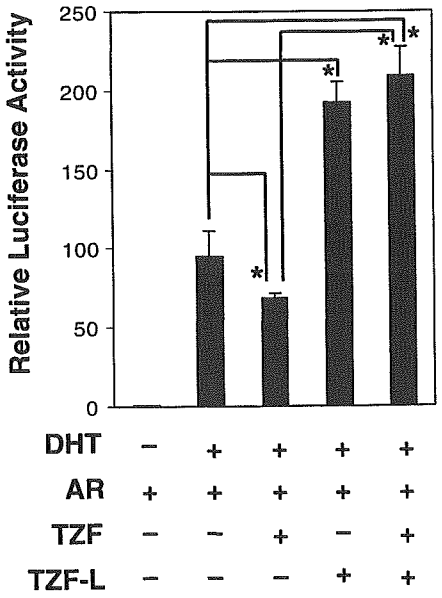

Fig. 3. TZF-L abrogates the repressive function of TZF on AR transactivation. COS-7 cells were transfected with pGL3-MMTV, pRL-CMV, pCMV-hAR, and the expression vector for TZF and/or TZF-L at equimolar amounts, and luciferase activity was measured after treatment with 10 nM DHT for 24 h as described in Materials and methods. Bars represent fold changes in luciferase activity relative to the value by AR without DHT. Data are represented means ± SD of three independent experiments. $*P < 0.01$.

immersion objective as described previously [14,15]. Images were collected at a 12-bit depth resolution of intensities over 1024 × 1024 pixels. For excitation of GFP and YFP, 488-nm argon lasers were employed, and emission signals were separated using the Emission Fingerprinting technique established by Carl Zeiss.

Results

TZF-L enhances AR-mediated transcriptional activation

We previously reported that TZF repressed AR-mediated transcriptional activation [11]. We also isolated an alternative spliced variant of TZF, TZF-L (2025 amino acid residues), which was much longer than TZF (942 amino acid residues) [10]. Nine hundreds and two N-terminal amino acid residues were common in these two variants. To examine effects of TZF-L on AR-mediated transactivation function, a functional reporter assay was performed using a PSA promoter in PC3 cells. Surprisingly, TZF-L enhanced ligand-induced transcriptional activation by AR in a dose-dependent fashion (Fig. 1). Using a different promoter (MMTV) and different cells (COS-7), a similar promoting effect by TZF-L on AR-mediated transactivation was observed (data not shown). These results revealed that, interestingly, TZF-L acted as a coactivator for AR in contrast with the corepressor function of TZF.

The N-terminus of TZF-L interacts with AR

As described previously, the N-terminal 902 amino acid residues of TZF-L were identical to those of TZF, which directly interacted with AR [11]. To examine the interaction of TZF-L with AR, a mammalian two-hybrid assay was performed using the full-length TZF-L and its deletion mutants, TZF-L-N and TZF-L-C, with AR (Fig. 2A). As shown in Fig. 2B, expressions of TZF-L and TZF-L-N but not of TZF-L-C showed higher activities compared to that of the negative control, demonstrating that TZF-L was able to interact with AR through its N-terminal domain. To further confirm the interaction of TZF-L with AR, immunoprecipitation analyses using AR with TZF-L or its mutants were carried out. As shown in Fig. 2C, AR was co-immunoprecipitated with full-length TZF-L and TZF-L-N, but not with TZF-L-C.

TZF-L completely abrogates the repression function of TZF on AR-mediated transactivation

TZF and TZF-L are alternative spliced proteins derived from one gene and are expressed in the same tissues and stages of spermatogenesis [10]. Such a pair of proteins often cooperates to regulate the same physiological processes. Here, we investigated effects of coexpression of these two proteins on AR-mediated transactivation. As shown in Fig. 3, TZF and TZF-L showed opposite effects on AR-mediated transactivation. Coexpression of TZF and TZF-L proteins promoted transactivation by AR to the same level as TZF-L alone. These results indicated that the suppressive effect of TZF

Fig. 4. Homo- and heterodimerization of TZF and TZF-L. (A) TZF forms homodimers and heterodimers with TZF-L. NIH3T3 cells were co-transfected with 0.6 μg pG5*luc*, 0.1 μg pBIND-TZF, and 0.3 μg pACT-TZF-L, pACT-TZF-L-N, or pACT-TZF-L-C. (B) Homodimerization of TZF is inhibited by TZF-L. NIH3T3 cells were transiently co-transfected with 0.3 μg pG5*luc*, 0.1 μg pBIND-TZF, and 0.2 μg pACT-TZF together with or without 1 μg pFLAG-CMV2-TZF or an equimolar amount of pFLAG-CMV2-TZF-L. (C) TZF-L forms homodimers. NIH3T3 cells were transiently co-transfected with 0.6 μg pG5*luc*, 3.3 ng pRL-CMV, 0.2 μg pBIND-TZF-L and 0.4 μg pACT-TZF-L. The cells were then incubated for 48 h and the luciferase activities were measured. Bars represent fold changes in luciferase activity relative to the value by the empty vectors. Data are represented means ± SD of three independent experiments. $*P < 0.01$. (D) TZF co-immunoprecipitates with TZF-L. COS-7 cells were transfected with 4 μg pFLAG-CMV2-TZF and 7.5 μg pEGFP-TZF-L or its empty vector. Whole cell lysates were immunoprecipitated using the anti-GFP antibody. Then, the precipitates were subjected to immunoblot analysis using the anti-TZF antibody for detection of TZF, or the anti-GFP antibody for detection of TZF-L. Whole cell lysates were also subjected to immunoblot analysis to confirm expression levels of TZF and GFP-TZF-L. (E) Distributions of TZF and TZF-L in living cells. COS-7 cells were transfected with pEYFP-TZF-L (a), pEGFP-TZF (b), pEGFP-TZF and pFLAG-CMV2-TZF-L (c), and pEYFP-TZF-L and pEGFP-TZF (d–f). After 24-h incubation, cells were observed using a LSM510META laser scanning microscope. For coexpression analysis, each fluorescent signal (d,e) was obtained using the Emission Fingerprinting technique as described in Materials and methods, and merged (f).

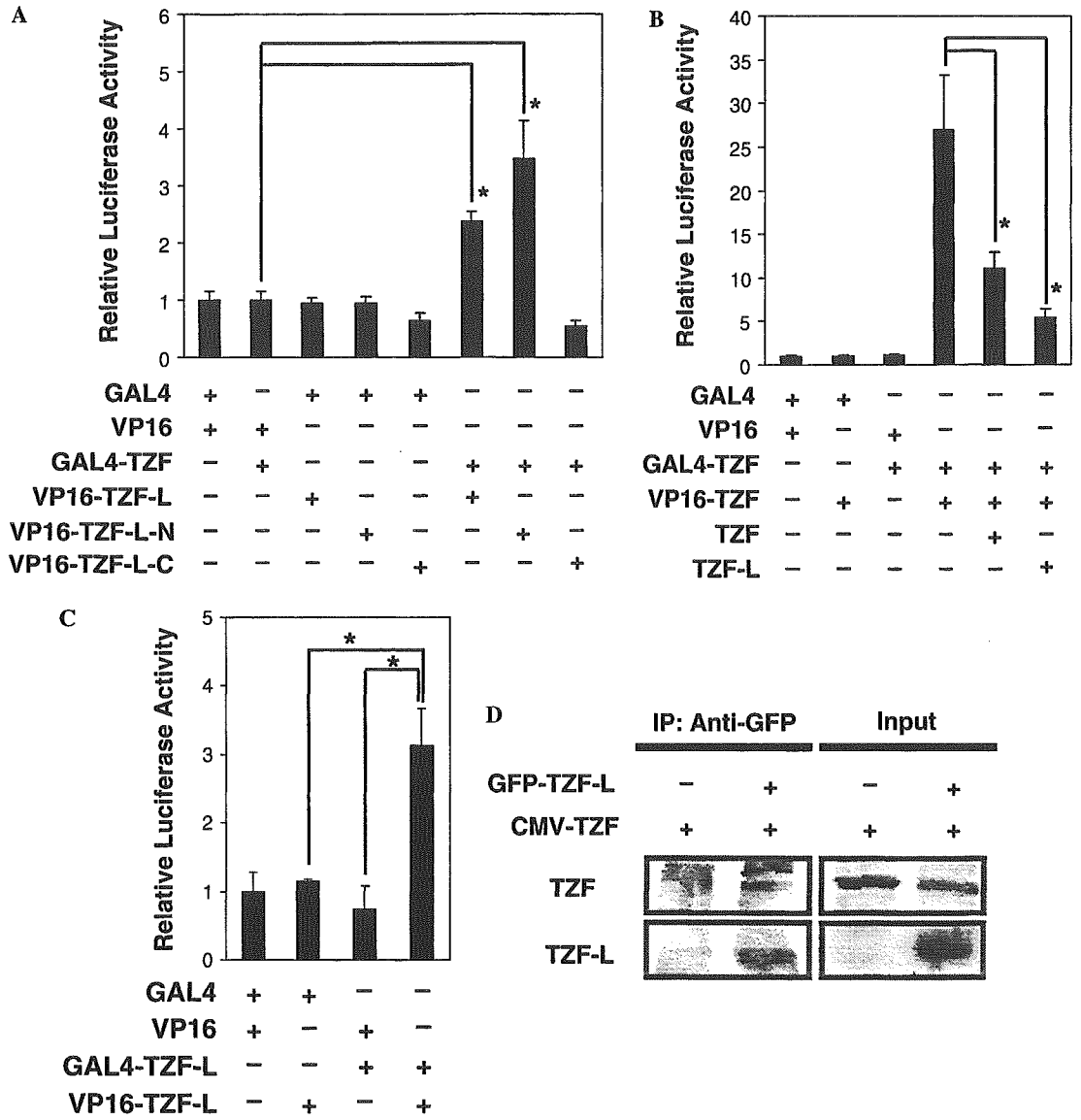
A
Relative Luciferase Activity
GAL4
VP16
GAL4-TZF
VP16-TZF-L
VP16-TZF-L-N
VP16-TZF-L-C
B
Relative Luciferase Activity
GAL4
VP16
GAL4-TZF
VP16-TZF
TZF
TZF-L
C
Relative Luciferase Activity
GAL4
VP16
GAL4-TZF-L
VP16-TZF-L
D
IP: Anti-GFP
Input
GFP-TZF-L
CMV-TZF
TZF
TZF-L
E
YFP-TZF-L
GFP-TZF
GFP-TZF
CMV-TZF-L
YFP-TZF-L
+
GFP-TZF
YFP-TZF-L
GFP-TZF
Merged

on AR-mediated transactivation was completely abrogated by coexpression of TZF-L.

TZF and TZF-L can form both homodimers and heterodimers

Abrogation of the TZF function by TZF-L made us wonder whether these two variants directly interacted with each other. To clarify this matter, a mammalian two-hybrid assay was performed. TZF was able to interact with full-length TZF-L and TZF-L-N, but not with TZF-L-C (Fig. 4A), indicating that TZF-L would form a heterodimer with TZF through its N-terminus. Further investigations suggested that TZF was able to form homodimers, which were strongly inhibited by coexpressing TZF and TZF-L (Fig. 4B). We also found that TZF-L formed homodimers (Fig. 4C). To confirm the interaction between TZF and TZF-L, a co-immunoprecipitation analysis was performed. TZF immunoprecipitated in the presence of anti-GFP antibody, only if GFP-TZF-L was coexpressed (Fig. 4D). Furthermore, we analyzed intracellular localizations of TZF and TZF-L using fluorescent proteins. As we previously reported, TZF formed discrete dots in the nucleus, whereas TZF-L seemed to be distributed at the euchromatin region (Figs. 4E, a and b) [10]. When GFP-TZF was coexpressed with non-fluorescent TZF-L, the intranuclear dots of TZF disappeared, and TZF showed the same intranuclear pattern as TZF-L, indicating that TZF was recruited to where TZF-L existed (Fig. 4E, c). Colocalization of TZF and TZF-L was confirmed using GFP-TZF and YFP-TZF-L (Figs. 4E, d–f). These data indicated that TZF and TZF-L formed both homodimers and heterodimers, and TZF-L recruited TZF.

Discussion

The two alternative spliced isoforms TZF and TZF-L showed opposite effects on AR-mediated transactivation as either corepressor or coactivator. We suggested that TZF was able to form not only homodimers but also heterodimers with TZF-L, and TZF-L inhibited homodimer formation of TZF. Furthermore, TZF-L formed homodimers. Based on these results, we propose a regulation mechanism for AR-mediated transactivation in which TZF homodimers act as corepressors, whereas TZF-TZF-L heterodimers and TZF-L homodimers act as coactivators for AR(Fig. 5).

We previously reported that both TZF and TZF-L were expressed at high levels in spermatogenic cells of testes. These results suggested that TZF and TZF-L might act to control gene activity at particular stages of spermatogenesis [10]. These two spliced variants showed similar stage-specific and tissue-specific expression patterns, suggesting that they functioned cooperatively.

TZF carries one zinc-finger motif, while TZF-L has two. The classical zinc-finger motif (C_2H_2-type) is one of the most common structural motifs in eukaryotes [16–18]. It is well

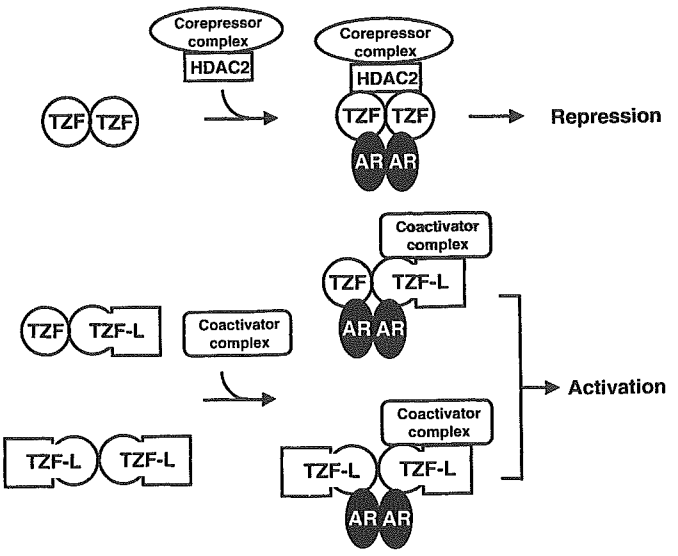

Fig. 5. A model for regulation of AR-mediated transactivation by TZF and TZF-L. Based on our experimental results, we propose a regulation mechanism for AR-mediated transactivation in which TZF homodimers act as corepressors, whereas TZF-TZF-L heterodimers and TZF-L homodimers act as coactivators for AR.

known that most zinc-finger proteins bind to cognate DNA and act as transcription factors. Recent studies revealed that many of these proteins are also able to mediate RNA binding and protein–protein interactions. A homology search for the two C_2H_2 zinc fingers of TZF-L revealed that these motifs were significantly homologous to those of U1 snRNP-specific protein C (U1C) family proteins [19,20]. U1C is critical to the initiation and regulation of pre-mRNA splicing, as a part of the U1 snRNP. In addition to this homology, TZF formed intranuclear dots which were closely located to those found for the splicing factor complex [11]. Based on these evidences, TZF and TZF-L might coordinate the splicing and transcription machineries to regulate nuclear receptor-mediated transactivation functions. Furthermore, U1C was reported to form homodimers through its C_2H_2 zinc-finger motif [21]. The zinc-finger motifs of TZF and TZF-L might also be important for homo- and heterodimerization of these proteins.

In the present study, we found that two alternative spliced variants of TZF had opposite effects on AR-mediated transcriptional activation. Among reported many coregulator proteins, CoAA (coactivator activator) and a short alternatively transcribed isoform, CoAM (coactivator modulator), also showed different actions on steroid hormone receptor-mediated transactivation [22,23]. CoAA, which was identified as a cofactor of thyroid hormone receptor-binding protein (TRBP), acts as a coactivator synergistically with TRBP and CBP [22]. In contrast, CoAM, which carries two RNA recognition motifs but lacks a TRBP-binding domain, completely eliminates synergistic activation effects of both TRBP and CBP. However, it is unclear whether CoAM just removes the CoAA-induced enhancement of the steroid hormone receptor-mediated

transactivation or acts as a corepressor for the steroid hormone receptor.

In conclusion, we identified a unique coregulator, TZF, whose two spliced isoforms functioned as coactivator or as corepressor. To our knowledge, this is the first study reporting that two spliced isoforms show reverse actions on NR-mediated transactivation.

Acknowledgments

This work was supported in part by Grants-in-Aid for Scientific Research (B) and Exploratory Research, and a grant for the 21st Century Center of Excellence (COE) Program(Kyushu University) from the Ministry of Education, Culture, Sports, Science and Technology, Japan.

References

[1] D.J. Mangelsdorf, C. Thummel, M. Beato, P. Herrlich, G. Schutz, K. Umesono, B. Blumberg, P. Kastner, M. Mark, P. Chambon, R.M. Evans, The nuclear receptor superfamily: the second decade, Cell 83 (1995) 835–839.

[2] A. Aranda, A. Pascual, Nuclear hormone receptors and gene expression, Physiol. Rev. 81 (2001) 1269–1304.

[3] A.O. Brinkmann, L.J. Blok, P.E. de Ruiter, P. Doesburg, K. Steketee, C.A. Berrevoets, J. Trapman, Mechanisms of androgen receptor activation and function, J. Steroid. Biochem. Mol. Biol. 69 (1999) 307–313.

[4] A.K. Roy, R.K. Tyagi, C.S. Song, Y. Lavrovsky, S.C. Ahn, T.S. Oh, B. Chatterjee, Androgen receptor: structural domains and functional dynamics after ligand-receptor interaction, Ann. N.Y. Acad. Sci. 949 (2001) 44–57.

[5] A. Tomura, K. Goto, H. Morinaga, M. Nomura, T. Okabe, T. Yanase, R. Takayanagi, H. Nawata, The subnuclear three-dimensional image analysis of androgen receptor fused to green fluorescence protein, J. Biol. Chem. 276 (2001) 28395–28401.

[6] M. Saitoh, R. Takayanagi, K. Goto, A. Fukamizu, A. Tomura, T. Yanase, H. Nawata, The presence of both the amino- and carboxyl-terminal domains in the AR is essential for the completion of a transcriptionally active form with coactivators and intranuclear compartmentalization common to the steroid hormone receptors: a three-dimensional imaging study, Mol. Endocrinol. 16 (2002) 694–706.

[7] C.A. Heinlein, C. Chang, Androgen receptor (AR) coregulators: an overview, Endocr. Rev. 23 (2002) 175–200.

[8] J.H. White, I. Fernandes, S. Mader, X.-J. Yang, Corepressor recruitment by agonist-bound nuclear receptors, Vitam. Horm. 68 (2004) 123–143.

[9] A. Inoue, A. Ishiji, S. Kasagi, M. Ishizuka, S. Hirose, T. Baba, H. Hagiwara, The transcript for a novel protein with a zinc finger motif is expressed at specific stages of mouse spermatogenesis, Biochem. Biophys. Res. Commun. 273 (2000) 398–403.

[10] M. Ishizuka, H. Ohshima, N. Tamura, T. Nakada, A. Inoue, S. Hirose, H. Hagiwara, Molecular cloning and characteristics of a novel zinc finger protein and its splice variant whose transcripts are expressed during spermatogenesis, Biochem. Biophys. Res. Commun. 301 (2003) 1079–1085.

[11] M. Ishizuka, H. Kawate, R. Takayanagi, H. Ohshima, R.-H. Tao, H. Hagiwara, A zinc finger protein TZF is a novel corepressor of androgen receptor, Biochem. Biophys. Res. Commun. 331 (2005) 1025–1031.

[12] M. Adachi, R. Takayanagi, A. Tomura, K. Imasaki, S. Kato, K. Goto, T. Yanase, S. Ikuyama, H. Nawata, Androgen-insensitivity syndrome as a possible coactivator disease, N. Engl. J. Med. 343 (2000) 856–862.

[13] G. Chen, M. Nomura, H. Morinaga, E. Matsubara, T. Okabe, K. Goto, T. Yanase, H. Zheng, J. Lu, H. Nawata, Modulation of androgen receptor transactivation by FoxH1: a newly identified androgen receptor corepressor, J. Biol. Chem. 280 (2005) 36355–36363.

[14] H. Kawate, Y. Wu, K. Ohnaka, H. Nawata, R. Takayanagi, Tob proteins suppress steroid hormone receptor-mediated transcriptional activation, Mol. Cell. Endocrinol. 230 (2005) 77–86.

[15] H. Kawate, Y. Wu, K. Ohnaka, R.-H. Tao, K.-I. Nakamura, T. Okabe, T. Yanase, H. Nawata, R. Takayanagi, Impaired nuclear translocation, nuclear matrix targeting and intranuclear mobility of mutant androgen receptors carrying amino acid substitutions in the DNA-binding domain derived from androgen insensitivity syndrome patients, J. Clin. Endocrinol. Metab. 90 (2005) 6162–6169.

[16] S. Iuchi, Three classes of C_2H_2 zinc finger proteins, CMLS. Cell. Mol. Life Sci. 58 (2001) 625–635.

[17] M. Ladomery, G. Dellaire, Multifunctional zinc finger proteins in development and disease, Ann. Hum. Genet. 66 (2002) 331–342.

[18] Y. Chen, G. Varani, Protein families and RNA recognition, FEBS J. 272 (2002) 2088–2097.

[19] R.L. Nelissen, V. Heinrichs, W.J. Habets, F. Simons, R. Lührmann, W.J. van Venrooij, Zinc finger-like structure in u1-specific protein C is essential for specific binding to U1 snRNP, Nucleic Acids Res. 19 (1991) 449–454.

[20] Y. Muto, D. Pomeranz Krummel, C. Oubridge, H. Hernandez, C.V. Robinson, D. Neuhaus, K. Nagai, The structure and biochemical properties of the human spliceosomal protein U1C, J. Mol. Biol. 341 (2004) 185–198.

[21] J.M. Gunnewiek, Y. van Aarssen, R. Wassenaar, P. Legrain, W.J. van enrooij, R.L. Nelissen, Homodimerization of the human U1 snRNP-specific pretein C, Nucleic Acids Res. 23 (1995) 4864–4871.

[22] T. Iwasaki, W.W. Chin, L. Ko, Identification and characterization of RPM-containing coactivator activator (CoAA) as TRBP-interacting protein, and its splice variant as a coactivator modulator (CoAM), J. Biol. Chem. 276 (2001) 33375–33383.

[23] D. Auboeuf, D.H. Dowhan, X. Li, K. Larkin, L. Ko, S.M. Berget, B.W. O'Malley, CoAA, a nuclear receptor coactivator protein at the interface of transcriptional coactivation and RNA splicing, Mol. Cell. Biol. 24 (2004) 442–453.

グルココルチコイドの骨代謝作用機構

高柳涼一*　大中佳三*

グルココルチコイド(GC)は生命現象の維持に必須のホルモンであるが，その過剰状態ではさまざまな副作用を引き起こす．GCは骨芽細胞の機能に対し二相性の作用を示す．生理量のGCは間葉系細胞の骨芽細胞系への分化と増殖を促進する．骨芽細胞の分化の極初期ではGCは転写因子PLZFの発現を誘導し，PLZFは転写因子Cbfa1を誘導し骨芽細胞前駆細胞の分化と増殖を促進する．一方，過剰量のGCは骨芽細胞の分化の後期を抑制，アポトーシスを誘導，局所での増殖因子の産生の抑制，さらにWntなどの骨形成シグナルを抑制して骨形成を抑制し，ステロイド性骨粗鬆症を惹起する．

Key words　グルココルチコイド，骨芽細胞，Wnt，骨形成抑制，骨粗鬆症

はじめに

副腎皮質より分泌されるステロイドホルモンであるグルココルチコイド(GC)は生命現象の維持に必須であるが，過剰状態ではさまざまな副作用を引き起こす．骨に対しても，生理量のGCは骨の分化・形成に必須であるが，過剰量のGCは骨形成を抑制し，ステロイド性骨粗鬆症を引き起こす．

本稿ではGCの骨組織に対する直接作用の最近の知見について，われわれの成績を含めて概説する．

GCとグルココルチコイド受容体(GR)の作用機構

GCの作用には古典的なgenomic作用に加えて，non-genomicな作用も近年注目されているが，骨代謝における後者の意義については十分に解明されてはいない．GCはグルココルチコイド受容体(GR)と結合してホモダイマーを形成し，標的遺伝子のプロモータ領域に存在するグルココルチコイド応答領域(GRE)に結合して転写を調節するtransactivation作用と，AP-1やNF-κBなどの転写因子とヘテロダイマーを形成することにより，抗炎症・抗免疫などの作用を示すtransrepression作用がある．GCの骨組織に対する作用はtransactivation作用と推定されている．GRにはαとβのサブタイプがあるが，正常の骨芽細胞にはGRαが発現しており，GCの作用はGRαを介すると考えられる．

GCによる骨分化促進作用

生理的濃度(1nM～10nMオーダー)のGCは，ラット骨

*TAKAYANAGI Ryoichi，OHNAKA Keizo/九州大学大学院医学研究院老年医学

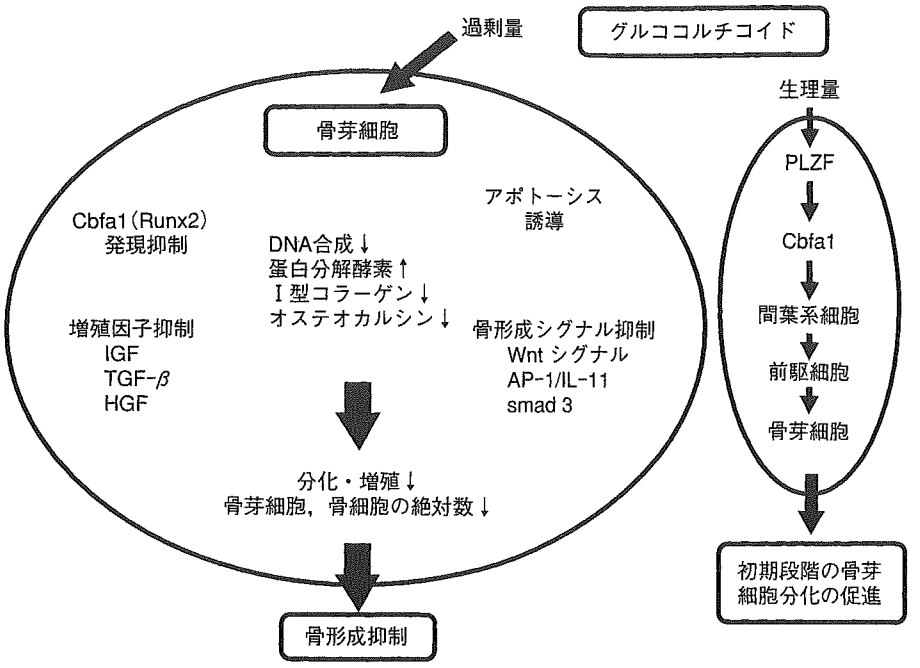

図❶ グルココルチコイドの骨芽細胞に対する二面性の作用機序
グルココルチコイド(GC)は骨芽細胞の分化増殖に対して二面性の作用を示す．骨芽細胞の分化の極初期ではGCは転写因子PLZFの発現を誘導し，PLZFは転写因子Cbfa1を誘導し骨芽細胞前駆細胞の分化と増殖を促進する．一方，過剰量のGCは骨芽細胞の分化の後期を抑制，アポトーシスを誘導，さらにWntなどの骨形成シグナルを抑制して骨形成を抑制する．

髄間質細胞の骨芽細胞系への分化を促進し[1]，ラット頭蓋冠由来の細胞のbone noduleの形成を促進する[2]．このGCの作用は骨芽細胞前駆細胞の分化と増殖を促進することによる[3]．

従来より実験的に，骨髄間葉系細胞を骨芽細胞へ分化させるのに，アスコルビン酸やグリセロリン酸に加えてGCが必須であることが知られていたが，その分子メカニズムは不明であった．最近，Ikedaら[4]はcDNAマイクロアレイ解析を用いて，後縦靱帯骨化症患者の靱帯細胞をデキサメタゾン，アスコルビン酸，β-グリセロリン酸で骨化誘導した際に発現が最も増加する遺伝子としてpromyelocytic leukemia zinc finger(*PLZF*)を同定した．PLZFはzinc finger protein 145(ZNF145)ともよばれるKrupple型のzinc finger domainをもつ転写因子であり，間葉系細胞から骨芽細胞への分化において，Cbfa1(Runx2)の上流で作用することが明らかになった．PLZFはデキサメタゾンにて発現が誘導されること，PLZFを欠くとCbfa1の誘導が消失するので，デキサメタゾンによる骨芽細胞の早期の分化に重要なはたらきをすることが示された(図❶)．

GCによる骨形成抑制作用

1) 骨芽細胞機能の抑制

過剰量(薬理量：100nMオーダー以上)のGCは骨芽細胞の増殖，分化を抑制する(図❶)．GCによる骨芽細胞の増殖抑制にはmitogen activated protein(MAP)キナーゼの抑制や細胞周期を制御する蛋白の抑制などが関与するが，MAPキナーゼの1つであるextracellular regulated kinase(ERK)を不活化するホスファターゼ(MKP-1)がGCにより骨芽細胞で著しく誘導されること[5]，チロシンホスファターゼ阻害剤がラットのステロイド性骨粗鬆症を予防すること[6]が報告されている．GCは骨芽細胞の分化に必須の転写因子であるCbfa1(Runx2)の発現を抑制する[7]．骨形成誘導作用を有するbone morphogenetic protein(BMP)-2も抑制することが知られている．また

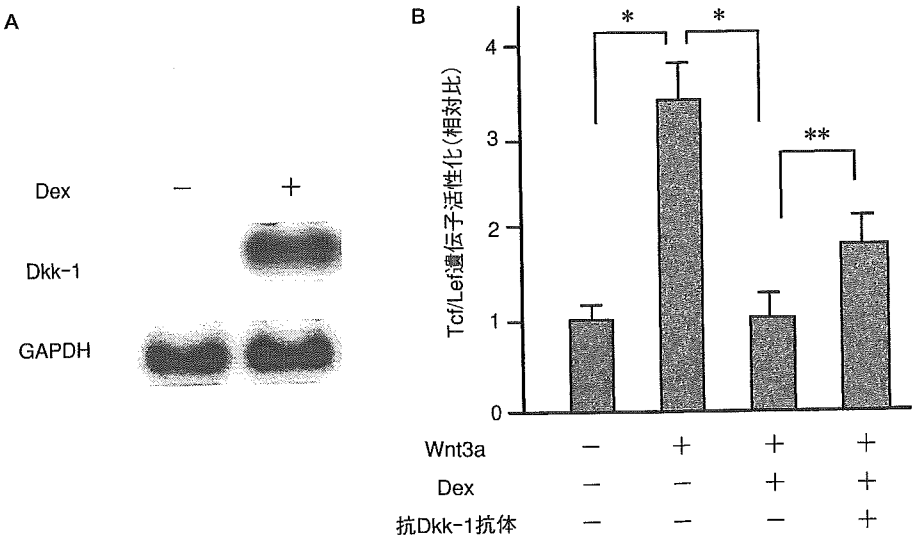

図❷ 培養ヒト骨芽細胞での10^{-7}M デキサメタゾン(Dex)によるDkk-1の発現増加とcanonical Wnt signalの抑制

A. DexはWntのアンタゴニストであるdickkopf-1(Dkk-1)の発現を強力に誘導する．
B. DexはWnt3aによるTcf/Lef応答性遺伝子の転写活性の亢進を完全に抑制するが，抗Dkk-1抗体の添加により，Dexによる転写抑制が部分的に回復される．
(*p＜0.01, **p＜0.05)

(Ohnaka K *et al*, 2004[22], Ohnaka K *et al*, 2005[23]より改変引用)

GCは間葉系細胞を骨芽細胞ではなく，脂肪細胞へ分化させるperoxisome proliferator-activated receptor(PPAR)γを増加させる[8]．GCは骨芽細胞のアポトーシスを促進するが，その機序としてBcl-2の発現低下とBaxの発現亢進によるBcl-2/Bax比の低下[9]が報告されている．ステロイド性骨粗鬆症のモデルマウスやプレドニゾロンを長期に内服しているヒトの骨組織の生検像でも，骨芽細胞のアポトーシスの亢進を認めている[10]．GCは骨芽細胞がつくる骨基質蛋白であるⅠ型コラーゲンやβ1インテグリンの産生を低下するとともに，コラーゲンを分解するコラゲナーゼ3(MMP-13)の産生を亢進させる[11]．また骨芽細胞の終分化の指標となるオステオカルシンの産生を転写レベルで抑制する[12]．

2) 局所産生因子への影響

GC は局所での増殖因子の産生にも影響を及ぼす．インスリン様成長因子(Insulin-like growth factor：IGF)は強力なanabolic作用を有する最も重要な局所調節因子の1つである．IGF-ⅠやIGF-Ⅱは弱いmitogen作用をもち，骨芽細胞のreplicationを促進する．またⅠ型コラーゲンを増加させ，コラゲナーゼ3を抑制する作用をもつ．GCは骨芽細胞のIGF-Ⅰ合成を低下させるが，その機序としてC/EBPβやC/EBPδの発現亢進を介した転写レベルでの抑制が関与する[13]．GCはIGF-Ⅱ受容体の発現を抑制し，IGF結合蛋白(IGFBP)-3，4，5を減少させ，その結果IGF作用を減弱させる[14]．Transforming growth factor(TGF)-βは骨芽細胞の増殖やコラーゲン合成を促進する増殖因子である．GCにより骨芽細胞からのTGF-βの発現量は変化しないものの，ライソゾームのプロテアーゼ産生が増加し，latent formのTGF-βが増加する結果，TGF-βの作用は低下する[15]．肝細胞増殖因子(HGF)は骨芽細胞の機能を刺激するとともに，骨吸収を強力に抑制する．GCは骨芽細胞からのHGFの産生を抑制することが報告されている[16]．

3) 骨形成シグナルへの影響

a. AP-1/IL-11経路

力学的負荷の低下や加齢に伴う骨形成の低下に関与するシグナル系の研究において，AP-1/インターロイキン(IL)-11経路が骨形成の維持に重要な役割を担うことが明らかにされている[17]．GCはこのAP-1/IL-11経路を抑制するため，骨形成を低下させる可能性がある．

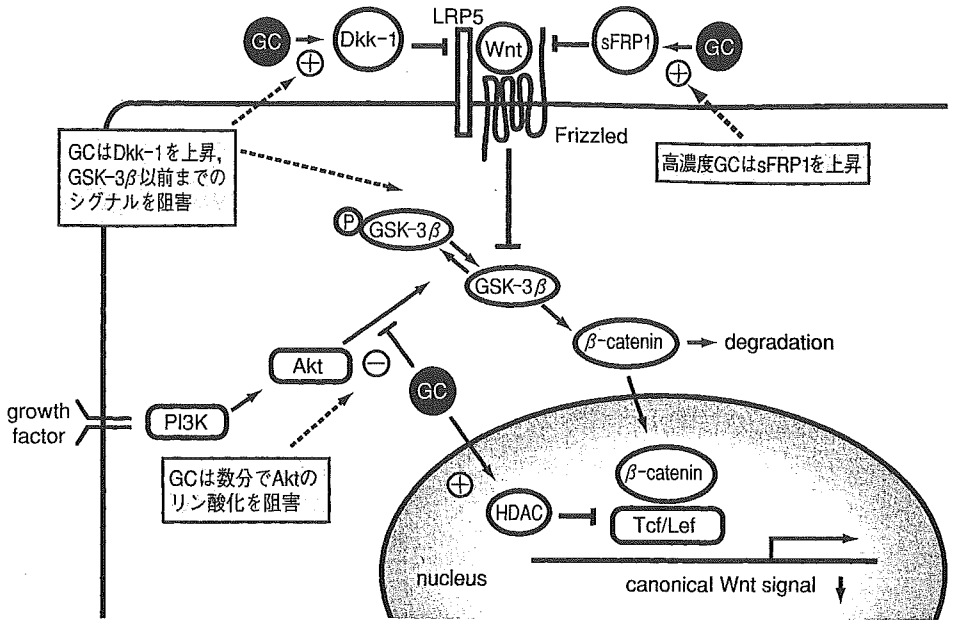

図❸ グルココルチコイドのWntシグナルへの影響
グルココルチコイドは骨芽細胞においてWntシグナルのアンタゴニストであるDkk-1やsFRP1の上昇や，WntシグナルによるGSK-3β活性の抑制を阻害することによりcanonical Wnt signalを抑制する．（高柳涼一ほか，2005[26]より改変引用）

b. Smad3経路

GCは培養骨芽細胞系においてSmad3依存性のALP活性やⅠ型コラーゲンの発現を抑制するが，この機序としてSmad3の発現を変化させるのではなく，Smad3による転写活性を抑制すること[18]が最近報告された．

c. Wntシグナル経路

Wntシグナルは胎生期の発生・分化と形態形成に加え，癌化やインスリン分泌不全・脂質代謝異常などの病態形成に関与する重要なシグナル伝達系である．Wntシグナルが骨形成に重要であることは，易骨折性を呈するosteoporosis-pseudoglioma症候群（OPPG）の原因が*LRP5*遺伝子のloss of function変異であったこと[19]，LRP5のノックアウトマウスでosteoporosisなどOPPGと同様のフェノタイプを呈したこと[20]，*LRP5*遺伝子のgain of function変異では逆に高い骨密度と口蓋外骨腫を呈するhigh bone massを発症すること[21]などから明らかになった．Wntシグナルによる骨形成は，骨の発生・分化に重要な転写因子Cbfa1（Runx2）の作用とは独立したものであり，出生後の骨量と骨強度の増加に重要であること[20]も明らかになった．したがって，成長後の骨に対して骨芽細胞の骨形成機能を強く抑制するGCがこのWntシグナル系に影響を及ぼす可能性が想定された．われわれ[22,23]はヒトの初代培養骨芽細胞において，臨床的に常用される量のGCがWntシグナルのcanonical経路を完全に抑制すること，この抑制にはLRP5に結合してWntシグナルを抑制するdickkopf-1（Dkk-1）の転写レベルでの著明な上昇と細胞内のGSK-3βまでの経路の抑制によることを見出した（図❷）．またGCによる別のWntアンタゴニストであるsecreted frizzled-related protein（sFRP）1の増加作用[24]や，nongenomicな経路を介したGSK-3βへの作用[25]も報告されている（図❸）[26]．GCによるWntシグナル系の抑制はステロイド性骨粗鬆症の発症に大きく関与している可能性があり，興味がもたれる．

GCの骨吸収と骨形成に対する作用

ヒトのステロイド性骨粗鬆症は，ステロイド投与初期の3～6ヵ月は急激に骨量が減少し，その後は緩やかな減少に移行する二相性を示す．マウスモデルの検討では急性期の骨組織では，骨芽細胞数は著しく減少し，骨芽細胞のアポトーシスが亢進していた．一方，破骨細胞数は増加しており，破骨細胞数/骨芽細胞数の比は骨密度低

下の割合とよく相関していた．すなわち，ステロイド投与初期は骨形成の急激な低下に加え，骨吸収の亢進により急激な骨量低下が起こることが示唆された[27]．慢性期の骨組織では，骨芽細胞数の減少とともに破骨細胞数も減少していた．すなわち，慢性期では骨形成，骨吸収ともに抑制され，骨代謝全体が低下するため，緩やかな骨量の低下をきたすことが示唆された[10]．このような骨代謝全体の抑制がヒトでもステロイド投与の慢性期に起こっていることを示す例として，クッシング症候群術後の骨代謝マーカーの検討の報告がある．副腎腫瘍摘出後，骨代謝マーカーは骨形成，骨吸収ともに術後3ヵ月以内に急激に正常域を超えて上昇し，以後緩やかに減少し正常化した[28]．この現象は，ステロイド過剰が慢性的に持続した状態では骨形成，骨吸収ともに強く抑制されており，急にステロイド過剰が解除されたために骨代謝全体のリバウンドが起こったものと推測される．ステロイドの投与量や期間により破骨細胞機能が変動することが原因と推定されるが，これまでの報告では，破骨細胞の骨吸収に対するステロイドの影響は一定の見解が得られていない．

おわりに

GCの骨組織に対する二面性の作用はおもに*in vitro*や動物実験にもとづいた成績に由来する．実際に，生理量のGCが骨形成を抑制しないかどうかの評価については，副腎不全であるAddison病の患者に対して補充量のGCを長期間投与したときの骨密度測定の成績が報告されている．最近は，補充量，すなわち，生理量のGCは骨密度を低下させないと報告されているが，GCの種類によっては骨密度低下が指摘されている[29][30]．また，骨折に対しては不明であり，骨質も含めて骨強度に影響しないかどうかの結論は得られていない．過剰量のGCによる骨芽細胞機能の抑制と骨形成の低下は，ステロイド性骨粗鬆症発症の主要なメカニズムであり，その分子機構をさらに明らかにすることが今後重要と考えられる．

文 献

1) Bellows CG, Aubin JE, Heersche JN : Physiological concentrations of glucocorticoids stimulate formation of bone nodules from isolated rat calvaria cells *in vitro*. *Endocrinology* **121** : 1985-1992, 1987
2) Leboy PS, Beresford JN, Devlin C *et al* : Dexamethasone induction of osteoblast mRNAs in rat marrow stromal cell cultures. *J Cell Physiol* **146** : 370-378, 1991
3) Tenenbaum HC, Heersche JN : Dexamethasone stimulates osteogenesis in chick periosteum *in vitro*. *Endocrinology* **117** : 2211-2217, 1985
4) Ikeda R, Yoshida K, Tsukahara S *et al* : The promyelotic leukemia zinc finger promotes osteoblastic differentiation of human mesenchymal stem cells as an upstream regulator of CBFA1. *J Biol Chem* **280** : 8523-8530, 2005
5) Engelbrecht Y, de Wet H, Horsch K *et al* : Glucocorticoids induce rapid up-regulation of mitogen-activated protein kinase phosphatase-1 and dephosphorylation of extracellular signal-regulated kinase and impair proliferation in human and mouse osteoblast cell lines. *Endocrinology* **144** : 412-422, 2003
6) Hulley PA, Conradie MM, Langeveldt CR *et al* : Glucocorticoid-induced osteoporosis in the rat is prevented by the tyrosine phosphatase inhibitor, sodium orthovanadate. *Bone* **31** : 220-229, 2002
7) Chang DJ, Ji C, Kim KK *et al* : Reduction in transforming growth factor beta receptor I expression and transcription factor CBFa1 on bone cells by glucocorticoid. *J Biol Chem* **273** : 4892-4896, 1998
8) Wu Z, Bucher NL, Farmer SR : Induction of peroxisome proliferator-activated receptor gamma during the conversion of 3T3 fibroblasts into adipocytes is mediated by C/EBPbeta, C/EBPdelta, and glucocorticoids. *Mol Cell Biol* **16** : 4128-4136, 1996
9) Gohel A, McCarthy MB, Gronowicz G : Estrogen prevents glucocorticoid-induced apoptosis in osteoblasts *in vivo* and *in vitro*. *Endocrinology* **140** : 5339-5347, 1999
10) Weinstein RS, Jilka RL, Parfitt AM *et al* : Inhibition of osteoblastogenesis and promotion of apoptosis of osteoblasts and osteocytes by glucocorticoids. *J Clin Invest* **102** : 274-282, 1998
11) Delany AM, Jeffrey JJ, Rydziel S *et al* : Cortisol increases interstitial collagenase expression in osteoblasts by post-transcriptional mechanisms. *J Biol Chem* **270** : 26607-26612, 1995
12) Aslam F, Shalhoub V, van Wijnen AJ *et al* : Contributions of distal and proximal promoter elements to glucocorticoid

regulation of osteocalcin gene transcription. *Mol Endocrinol* **9** : 679-690, 1995

13) Delany AM, Durant D, Canalis E : Glucocorticoid suppression of IGF I transcription in osteoblasts. *Mol Endocrinol* **15** : 1781-1789, 2001

14) Gabbitas B, Pash JM, Delany AM *et al* : Cortisol inhibits the synthesis of insulin-like growth factor-binding protein-5 in bone cell cultures by transcriptional mechanisms. *J Biol Chem* **271** : 9033-9038, 1996

15) Oursler MJ, Riggs BL, Spelsberg TC : Glucocorticoid-induced activation of latent transforming growth factor-beta by normal human osteoblast-like cells. *Endocrinology* **133** : 2187-2196, 1993

16) Skrtic S, Ohlsson C : Cortisol decreases hepatocyte growth factor levels in human osteoblast-like cells. *Calcif Tissue Int* **66** : 108-112, 2000

17) Tohjima E, Inoue D, Yamamoto N *et al* : Decreased AP-1 activity and interleukin-11 expression by bone marrow stromal cells may be associated with impaired bone formation in aged mice. *J Bone Miner Res* **18** : 1461-1470, 2003

18) Iu MF, Kaji H, Sowa H *et al* : Dexamethasone suppresses Smad3 pathway in osteoblastic cells. *J Endocrinol* **185** : 131-138, 2005

19) Gong Y, Slee RB, Fukai N *et al* : LDL receptor-related protein 5 (LRP5) affects bone accrual and eye development. *Cell* **107** : 513-523, 2001

20) Kato M, Patel MS, Levasseur R *et al* : Cbfa1-independent decrease in osteoblast proliferation, osteopenia, and persistent embryonic eye vascularization in mice deficient in Lrp5, a Wnt coreceptor. *J Cell Biol* **157** : 303-314, 2002

21) Boyden LM, Mao J, Belsky J *et al* : High bone density due to a mutation in LDL-receptor-related protein 5. *N Engl J Med* **346** : 1513-1521, 2002

22) Ohnaka K, Taniguchi H, Kawate H *et al* : Glucocorticoid enhances the expression of dickkopf-1 in human osteoblasts : novel mechanism of glucocorticoid-induced osteoporosis. *Biochem Biophys Res Commun* **318** : 259-264, 2004

23) Ohnaka K, Tanabe M, Kawate H *et al* : Glucocorticoid suppresses the canonical Wnt signal in cultured human osteoblasts. *Biochem Biophys Res Commun* **329** : 177-181, 2005

24) Wang FS, Lin CL, Chen YJ *et al* : Secreted frizzled-related protein 1 modulates glucocorticoid attenuation of osteogenic activities and bone mass. *Endocrinology* **146** : 2415-2423, 2005

25) Smith E, Frenkel B : Glucocorticoids inhibit the transcriptional activity of LEF/TCF in differentiating osteoblasts in a glycogen synthase kinase-3beta-dependent and-independent manner. *J Biol Chem* **280** : 2388-2394, 2005

26) 高柳涼一，大中佳三：ステロイド性骨粗鬆症．ファーマナビゲーター ビスフォスフォネート編，松本俊夫監修，メディカルレビュー社，大阪，2005，p.64-77

27) Weinstein RS, Chen J, Powers CC *et al* : Promotion of osteoclast survival and antagonism of bisphosphonate-induced osteoclast apoptosis by glucocorticoids. *J Clin Invest* **109** : 1041-1048, 2002

28) Hermus AR, Smals AG, Swinkels LM *et al* : Bone mineral density and bone turnover before and after surgical cure of Cushing's syndrome. *J Clin Endocrinol Metab* **80** : 2859-2865, 1995

29) Jodar E, Valdepenas MP, Martinez G *et al* : Long-term follow-up of bone mineral density in Addison's disease. *Clin Endocrinol* (*Oxf*) **58** : 617-620, 2003

30) Zelissen PM, Croughs RJ, van Rijk PP *et al* : Effect of glucocorticoid replacement therapy on bone mineral density in patients with Addison disease. *Ann Intern Med* **120** : 207-210, 1994

たかやなぎ・りょういち

高柳涼一　九州大学大学院医学研究院老年医学教授

福岡県生まれ．
専門は，老年医学，内分泌代謝学．
研究テーマは，骨粗鬆症，核内受容体，生活習慣病．

内分泌・糖尿病科，22(2)：147-152，2006

特集 骨粗鬆症治療の最前線

骨粗鬆症の病型 —老人性骨粗鬆症*

河手久弥**
高柳涼一**

Key Words : senile osteoporosis, involutional osteoporosis, estrogen, hip fracture

はじめに

わが国において骨粗鬆症に罹患している人は，すでに1,200万人を超えるものと推定され，さらなる高齢社会の進行に伴い，今後ますます骨粗鬆症患者数は増加するものと予想される．骨粗鬆症に伴う骨折は，加齢とともにその発生頻度が高くなり，高齢者の日常生活動作(ADL)やquality of life(QOL)を著しく低下させ，さらには死亡率の上昇に繋がるため，高齢者骨粗鬆症患者の骨折をどのようにして予防するかがきわめて重要である．老人性骨粗鬆症は，70歳以上の男女に認められる，骨形成の低下，低代謝回転などを特徴とする骨粗鬆症として，これまでは閉経後のエストロゲン欠乏による急激な骨量減少に起因する閉経後骨粗鬆症と区別して考えられていた．しかし，高齢者の骨粗鬆症や男性骨粗鬆症においても，閉経後骨粗鬆症と同様に，エストロゲン欠乏が重要な発症要因になることが次々に報告され，これまでの分類を見直す動きが主流になりつつある．本稿では，高齢者における骨粗鬆症の病態および病型分類について概説する．

加齢と骨粗鬆症

骨粗鬆症は加齢とともにその有病率が増加する．日本骨代謝学会の診断基準を適用すると，70歳代女性で50%，80歳代女性では実に60%の人が骨粗鬆症患者であり[1]，わが国の骨粗鬆症患者の総数は現時点で1,200万人を超えるものと推計され，今後の高齢化の進展とともに，さらに骨粗鬆症患者数は増え続けるものと予想される．

ヒトの骨量は成長とともに増加し，20歳代にピーク(最大骨量)になり40歳前後までは維持されるが，その後は加齢とともに減少する．女性ではエストロゲンの枯渇により，閉経後の10～15年は急激な骨量減少を認めるが，その後は緩やかな減少にシフトする[2][3](図1)．男性では，65歳ごろから高齢の女性と同様の緩徐な骨量減少のみが続く．男性では，閉経後女性にみられるような急激な骨量減少がないことに加え，最大骨量が女性よりも大きいため，女性と比べて高齢になってから骨粗鬆症を発症する場合が多い．

高齢者の骨粗鬆症に伴う骨折の臨床的特徴

骨粗鬆症の重大な合併症は骨折であるが，椎体骨折や大腿骨頸部骨折の発生率も，年齢が高くなるに従って増加する[4]～[7](図2)．骨折リスクの評価には骨量の測定が重要で，骨量が低いと

* Classification of osteoporosis－senile osteoporosis.

** Hisaya KAWATE, M.D., Ph.D. & Ryoichi TAKAYANAGI, M.D., Ph.D.: 九州大学大学院医学研究院老年医学〔〒812-8582 福岡市東区馬出3-1-1〕; Department of Geriatric Medicine, Graduate School of Medical Sciences, Kyushu University, Fukuoka 812-8582, JAPAN

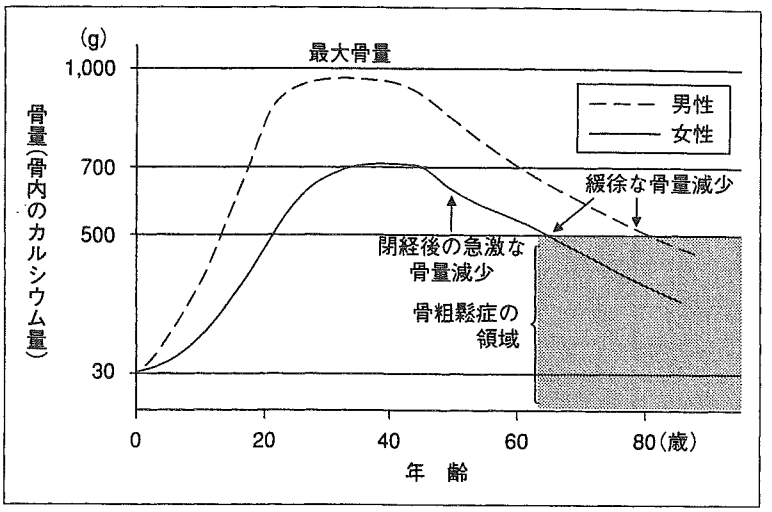

図1 加齢に伴う骨量の変化（文献[2)3)]より引用改変）

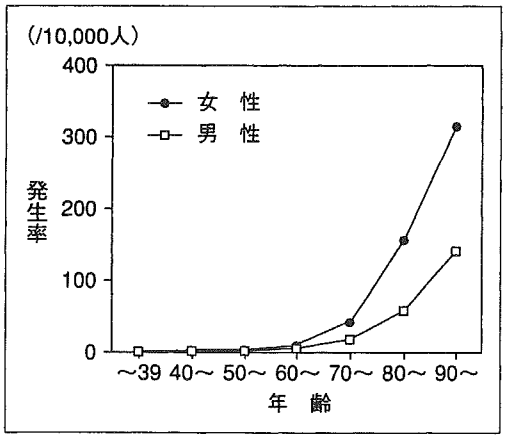

図2 大腿骨頸部骨折の性・年齢別発生率
（文献[7)]より引用改変）

表1 大腿骨頸部骨折のリスクファクター

年齢
低骨量
やせ(低BMI)
50歳以降の骨折の既往
大腿骨頸部骨折の家族歴
喫煙
ステロイド使用歴
アルコール多飲
リウマチ

（文献[8)]より引用改変）

将来骨折を起こす可能性が高くなる．しかしながら，高齢者では，骨量が正常であるにもかかわらず，骨折を起こす症例がしばしば認められる．統計学的にも骨折の発生率に関して，年齢は骨量とは独立の危険因子であり，同じ骨量でも年齢が高くなればなるほど，骨折の危険性が高くなることが示されている[6)8)]．高齢者で，とくにリスクファクター〔やせ，骨折の既往，大腿骨頸部骨折の家族歴，喫煙など[9)]（表1）〕を有する人に対しては，十分な骨折予防対策を施す必要がある．

高齢者では，大腿骨頸部骨折の発生率が高くなることが知られている（図2）．わが国では年間約12万人が新たに発症し，寝たきりの原因としては脳卒中に次いで第2位を占め，年々増加傾向にある．大腿骨頸部骨折を起こすと，ADLやQOLを著しく低下させるだけでなく，死亡率も上昇する．一方，椎体骨折の発生頻度は大腿骨頸部骨折より高いものの，臨床症状を伴うものは約3割に過ぎず，残りの約7割は痛みを伴わないため見過ごされることが多く，身長短縮や円背などの脊椎変形を起こして初めて気づかれることも多い．ところが，既存の椎体骨折を有する人は，骨折をしていない人と比べて，新たな椎体骨折を生じる危険性が高まる．さらに椎体骨折の数が増えるに従って生命予後が悪くなるという報告があり[10)11)]，既存の椎体骨折を認める場合は，無症状でも次の椎体骨折を予防するために，積極的な治療を行うことが必要である．